A unification scheme of pulsar inner- and outer- gap models

Kouichi HIROTANI

TIARA, Taiwan

Bad Honnef
May 16, 2006

The seven highest-confidence γ-ray pulsars

by CGRO

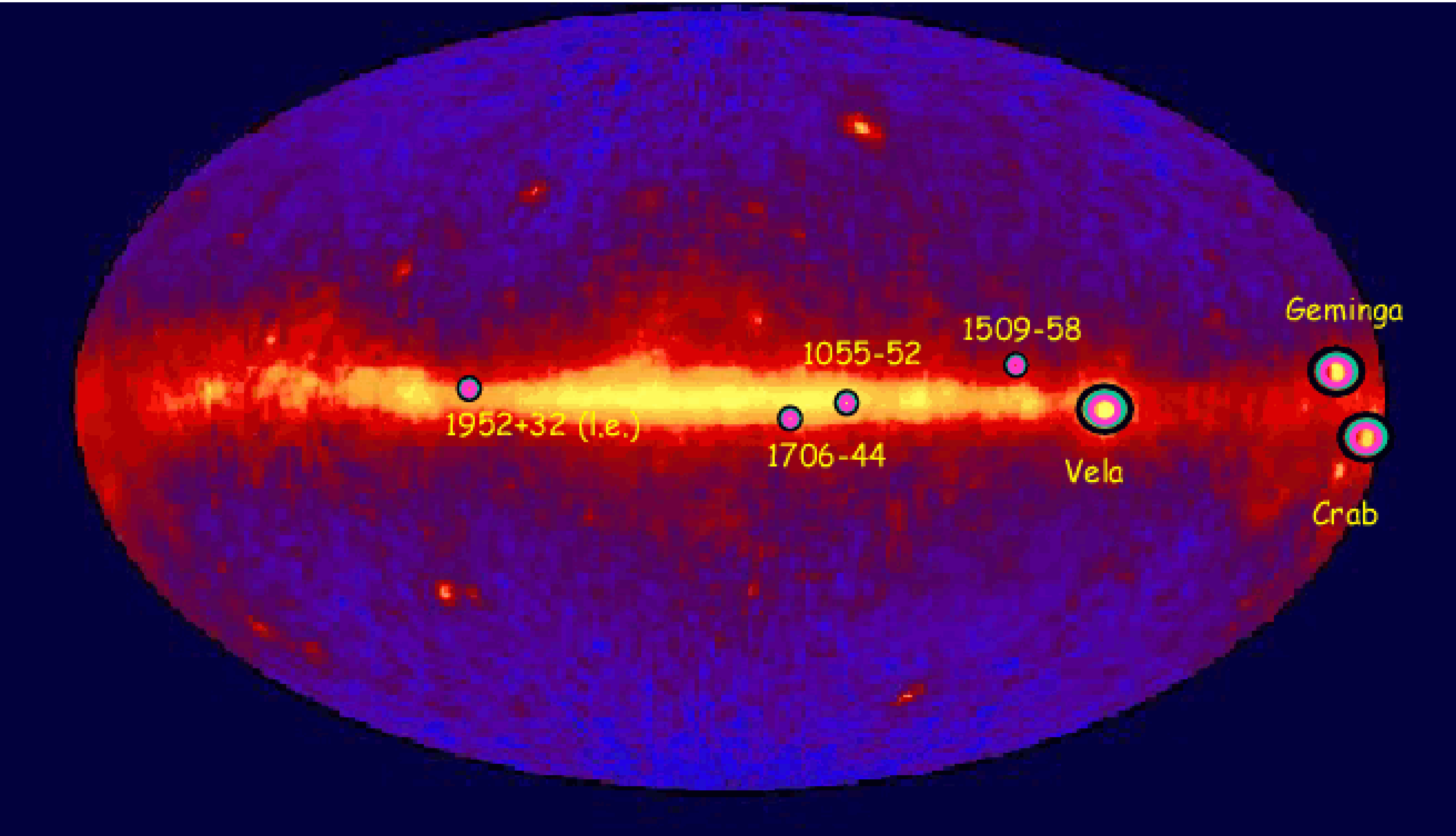

§1 Introduction: CGRO observations

High-energy lightcurves (>100 MeV)

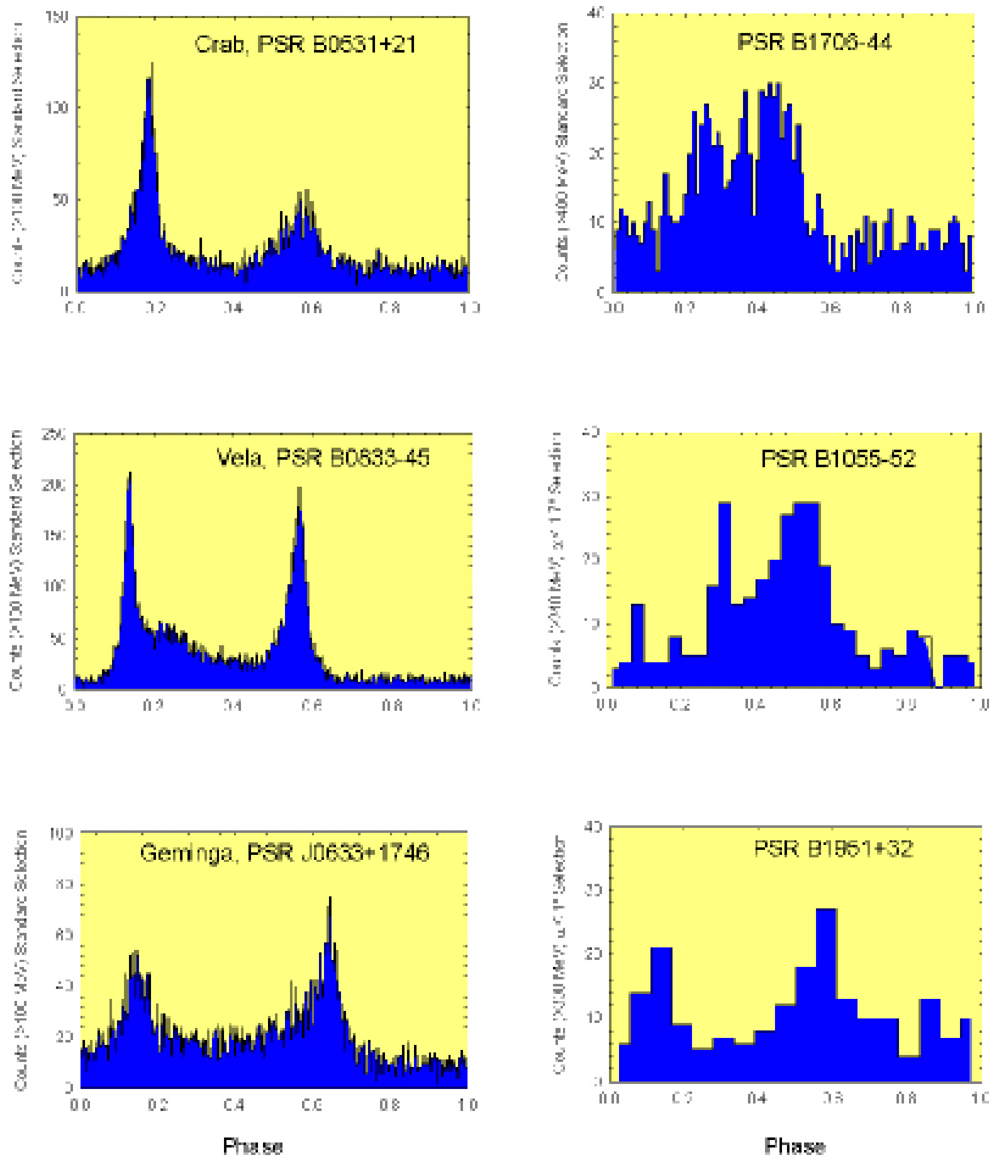

Kanbach (2002)
MPE report 278, 91

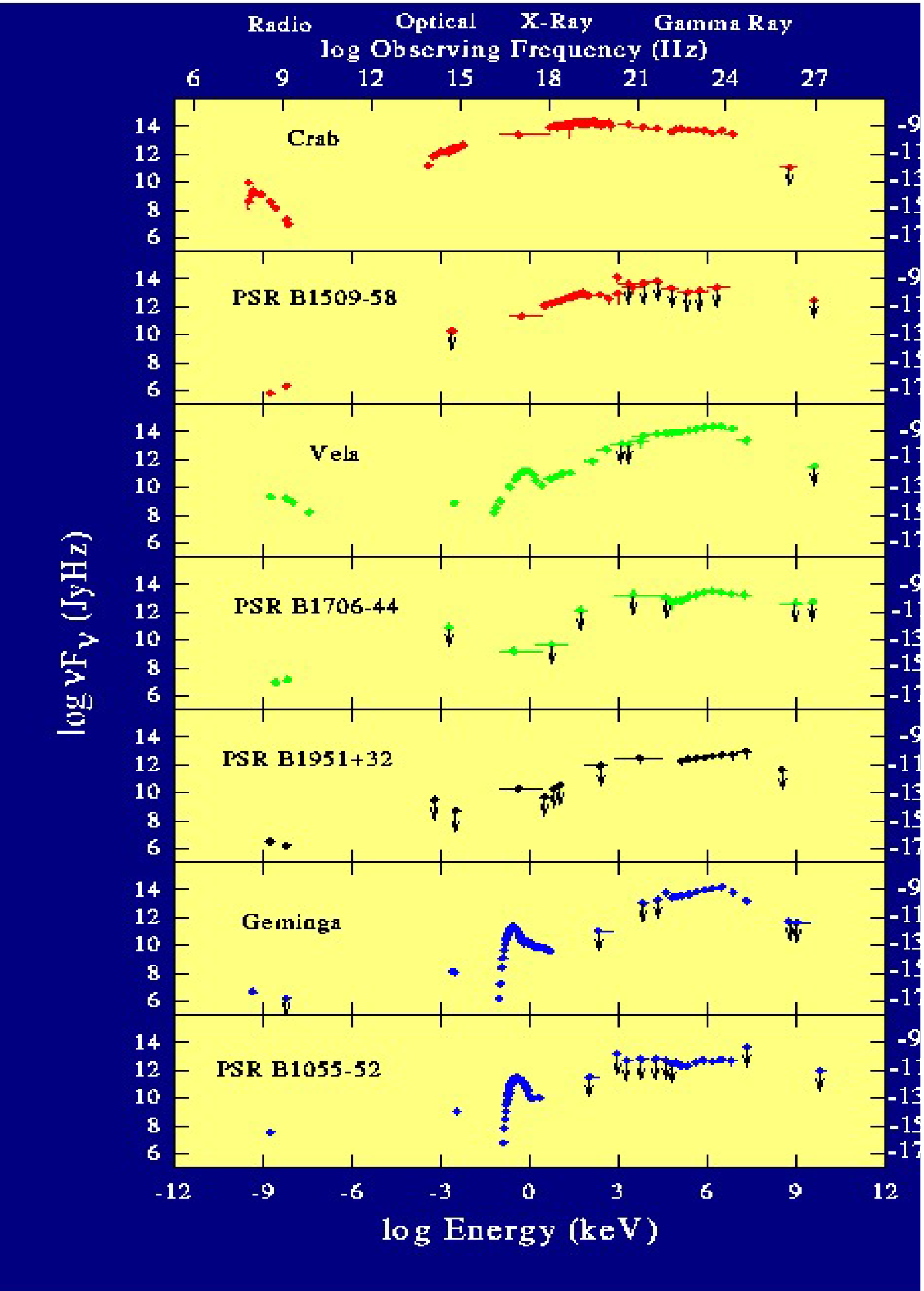

Broad-band spectra

High-energy (>100MeV) pulsed photons are emitted by ultra-relativistic (~10 TeV) e^-'s/e^+'s accelerated in pulsar magnetosphere via curvature process.

Thompson et al. (1999) ApJ 516, 297

§1 Intro.: Pulsar as a unipolar inductor

Where is the particle accelerator?

§2 *Accelerator Models*

A long-standing issue:

Inner-gap model

vs.

Outer-gap model

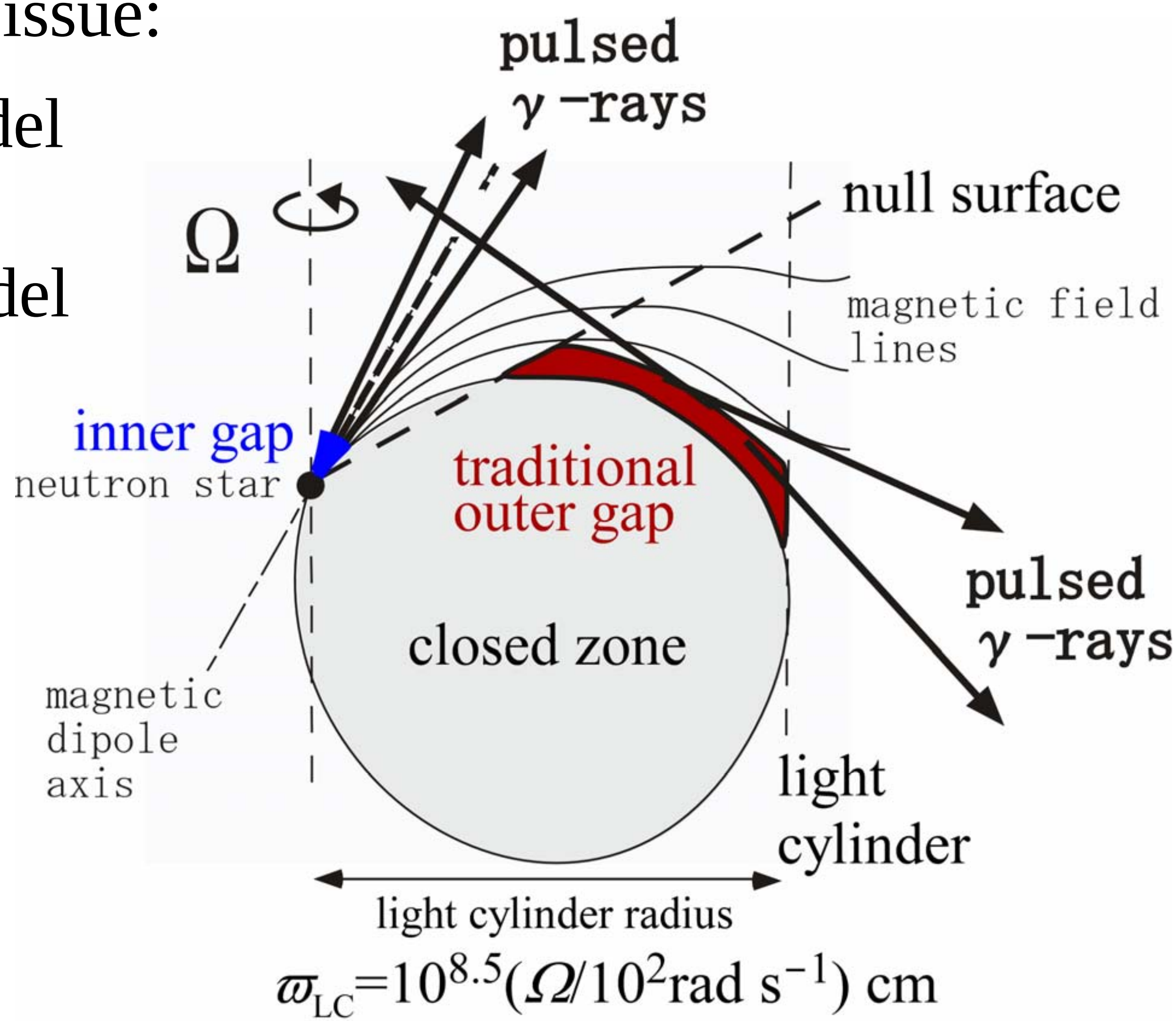

Fig. Two magnetospheric accelerators.

§2 *Accelerator models (cont’d)*

The modulation of the GeV light curves

High-Energy Lightcurves

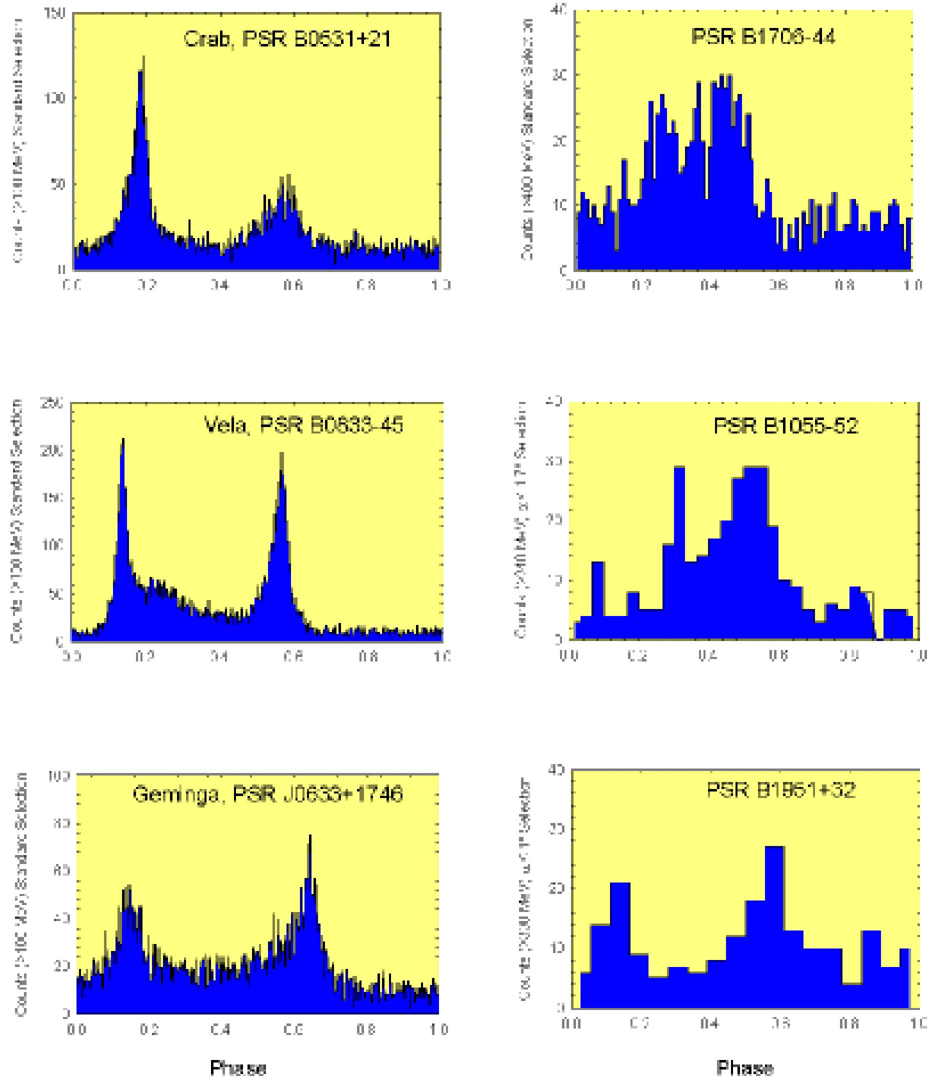

§2 Accelerator models (cont'd)

The modulation of the GeV light curves testifies to the -ray production at…

(1) inner gap (Harding et al. 1978, ApJ 225, 226;
Daugherty & Harding 1982 ApJ 252, 337;
1996 ApJ 458, 278;
Sterner et al. 1995, ApJ 445, 736),

(2) slot gap (Arons 1983, ApJ 302, 301;
Muslimov, Harding 2004, ApJ 606, 1143)

(3) outer gap (Cheng, Ho, Ruderman 1986, ApJ 300, 500;
300, 522
Romani, Yadigaroglu 1995, ApJ 438, 341)

(4) wind region (Kirk, Skjaeraasen 2002, AA 388, L29;
Petri, Kirk 2005, ApJ 627, L37)

§2 *Accelerator models (cont'd)*

Kirk and Petri will talk about (4) in the afternoon. So, let's concentrate on the radiation within light cylinder.

(1) inner gap (Harding et al. 1978, ApJ 225, 226;
Daugherty & Harding 1982 ApJ 252, 337;
1996 ApJ 458, 278;
Sterner et al. 1995, ApJ 445, 736),

(2) slot gap (Arons 1983, ApJ 302, 301;
Muslimov, Harding 2004, ApJ 606, 1143)

(3) outer gap (Cheng, Ho, Ruderman 1986, ApJ 300, 500;
300, 522
Romani, Yadigaroglu 1995, ApJ 438, 341)

(4) wind region (Kirk, Skjaeraasen 2002, AA 388, L29;
Petri, Kirk 2005, ApJ 627, L37)

§2 *Accelerator models (cont'd)*

(1) Inner-gap model (from lower altitudes, $s < 3\,r_*$)

A single inner-gap beam produces various pulse profiles with any peak separation between 0^o and 180^o.

However, one has to assume a small inclination and a lucky viewing angle ($\alpha \sim \zeta < 30^o$).

Seeking the possibility of a wide hollow cone emission due to flaring ***B*** field lines, Dyks & Rudak (2003) proposed the two-pole caustic model. Assuming a uniform emissivity along the last-open ***B*** field lines in $0 < s < \varpi_{\rm LC}$, they predict that double peaks arise from the crossing of caustics associated with both poles.

§2 Accelerator models (cont'd)

(2) Slot-gap model ($0 < s < \varpi_{\rm LC}$)

Dyks, Harding, Rudak (2004) explained the phase-aligned pulse profiles for the Crab pulsar and the formation of double peaks and off-pulse emission.

To give the physical basis of their two-pole caustic model, Muslimov & Harding (2003; 2004) revised the original slot-gap model (Arons 1983), by adding GR effects and $E_{||}$ screening due to gap narrowness at higher altitudes.

$\longrightarrow$ a gap solution extended from the NS surface to the outer magnetosphere.

§2 Slot gap model: problem

However, their slot gap (outward extension of the inner-gap model) predicts a negative $E_{||}$ when $\boldsymbol{\Omega}\bullet\boldsymbol{\mu} > 0$, which induces an opposite gap current from the global current flow patterns.

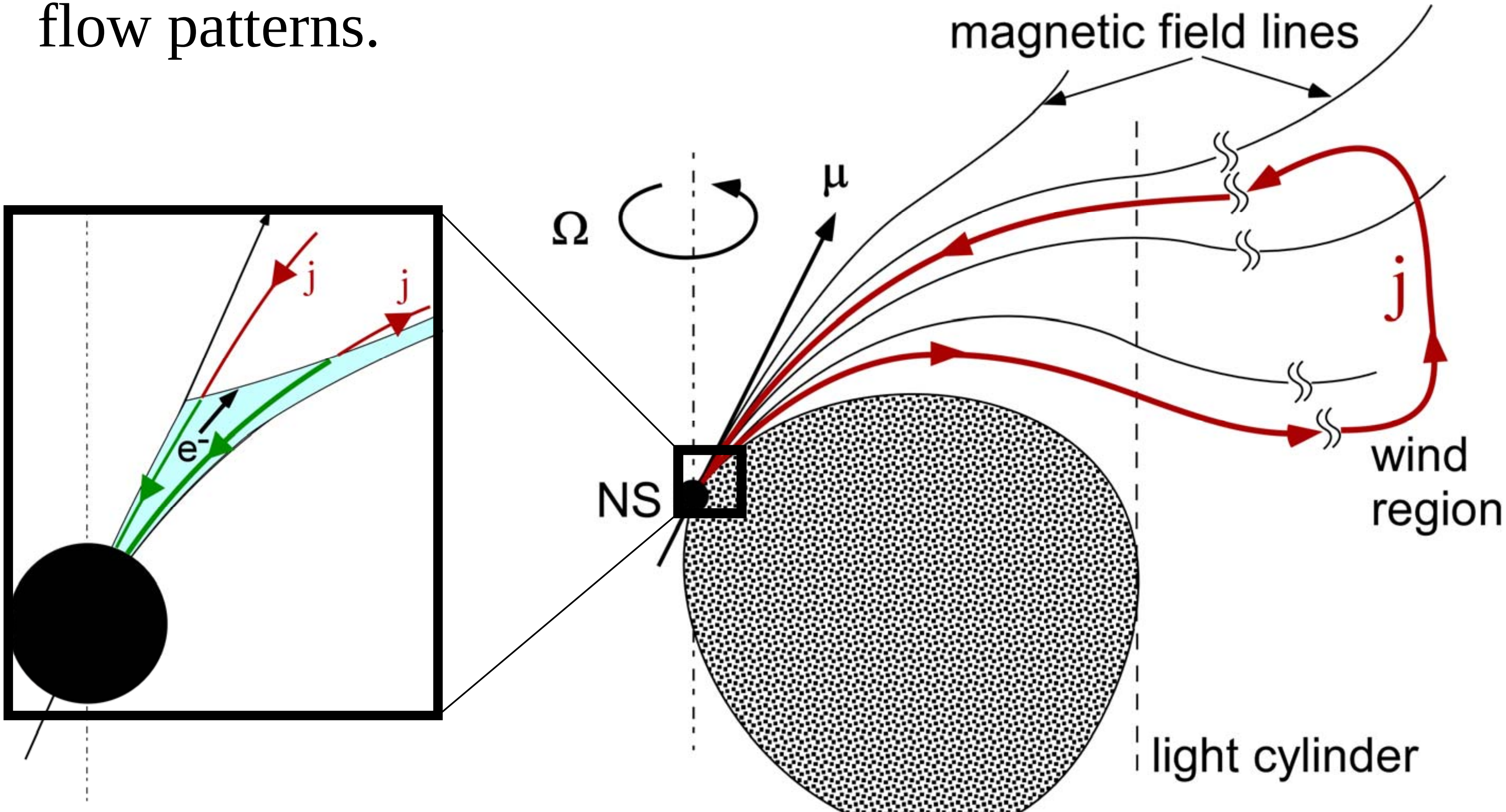

§2 Slot gap model: problems

However, their slot gap (outward extension of the inner-gap model) predict a negative $E_{||}$ when $\mathbf{\Omega} \cdot \boldsymbol{\mu} > 0$, which induces an opposite gap current from the global current flow patterns.

Outer-gap models, on the other hand, generally predict a positive $E_{||}$, which exerts consistent currents with global requirement.

→ Inward extension of the outer-gap model is an alternative way to consider an extended particle accelerator in pulsar magnetospheres.

§3 New accelerator model

To this aim, I solve the set of Maxwell & Boltzmann equations in pulsar magnetospheres on 2-D poloidal plane from the NS surface to the outer magnetosphere, extending modern outer-gap models

(Hirotani, Harding, Shibata 2003 ApJ 591, 334)

(Takata et al. 2006 MNRAS 366, 1310)

See also

Beskin et al. 1992, Sov. Astron. 36(6), 642

for the original idea applied to a BH magnetosphere.

§3 *New accelerator model*

Let us first describe the physical processes that take part in a stationary particle accelerator.

e^+ and e^- are accelerated by $E_{\|}$

Relativistic e^+/e^- emit γ-rays via synchro-curvature, and IC processes

γ-rays collide with soft photons or $\boldsymbol{B}$ to materialize as pairs in the accelerator

§3 New gap model: Maxwell equation

The Poisson equation for the electrostatic potential Ψ:

$$-\nabla^2\psi = 4\pi(\rho - \rho_{\mathrm{GJ}}) \,,$$

Boltzmann eqs. for e$^-$/e$^+$:

$$\frac{\partial N_\pm}{\partial t} + \mathbf{v}\cdot\nabla N_\pm + \left(e\mathbf{E}_\parallel + \frac{\mathbf{v}}{c}\times\mathbf{B} \right)\cdot\frac{\partial N_\pm}{\partial \mathbf{p}}$$

$$= \text{(IC+creation) collision terms}$$

Boltzmann eqs. for γ-rays:

$$\frac{\partial G}{\partial t} + c\frac{\mathbf{k}}{|\mathbf{k}|}\cdot\nabla G(t,\mathbf{x},E_\gamma,\mathbf{k}) = -(\eta_{\gamma\gamma} + \eta_{\gamma\mathrm{B}})G(t,\mathbf{x},E_\gamma,\mathbf{k})$$

$$+\int_1^\infty d\Gamma\ \left[\eta_{\mathrm{IC}\pm}(t,\mathbf{x},E_\gamma,\Gamma) + \eta_{\mathrm{SC}\pm}(t,\mathbf{x},E_\gamma,\Gamma)\right] N_\pm$$

§3 New accelerator model

We impose a stationary condition:

$$\frac{\partial}{\partial t} + \Omega \frac{\partial}{\partial \phi} = 0$$

To solve the Boltzmann equations.

§3 New accelerator model

Three free parameters:

- magnetic inclination (e.g., 45^o, 75^o),
- magnetic dipole moment of NS (e.g., $4*10^{30}$ G cm^3)
- trans-field gap thickness, h_m

Solve Poisson eq. + Boltzmann eqs. in 2+2 dim.

Imposing appropriate BDCs, we can solve

- gap geometry on the 2-D poloidal plane,
- $E_{||}(s,z)$ distribution,
- particle density and energy spectrum,
- γ-ray flux and energy spectrum,
- pair creation rate outside of the gap,

by specifying these three free parameters.

§4 *Application to the Crab Pulsar*

I applied the theory to the Crab pulsar.

§4 *Crab Pulsar: sub-GJ current solution*

If the gap is transversely thin, it is nearly vacuum.
(i.e., created current << Goldreich-Julian value)

→ Traditional outer-gap solution is obtained.
(e.g., $E_{\parallel}$ is nearly constant.)

$h_{\mathrm{m}} = 0.047$

mag. incl.
$\alpha = 70^{\circ}$

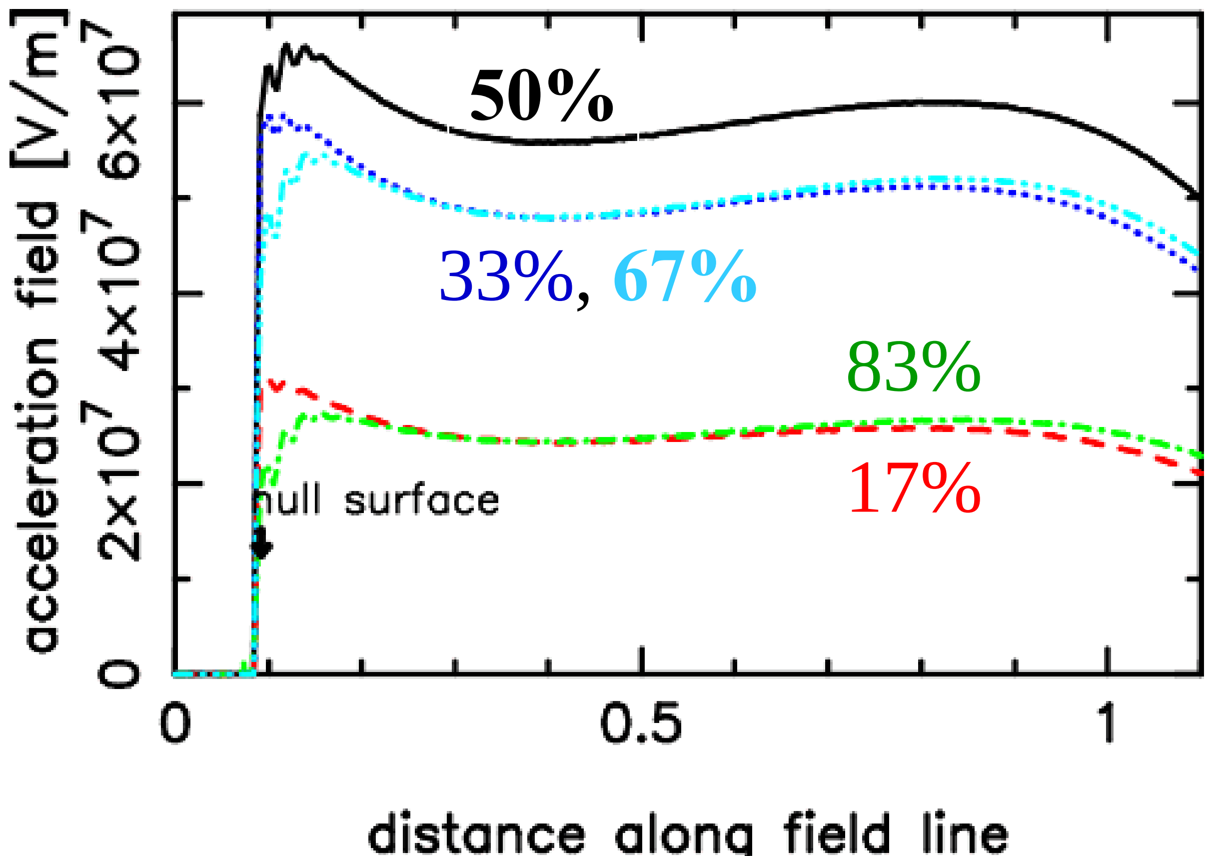

§4 sub-GJ solution: insufficient γ-ray flux

However, for the Crab pulsar, sub-GJ solution (i. e., traditional outer-gap model) predicts too small γ-ray flux.

Predicted phase-averaged spectrum

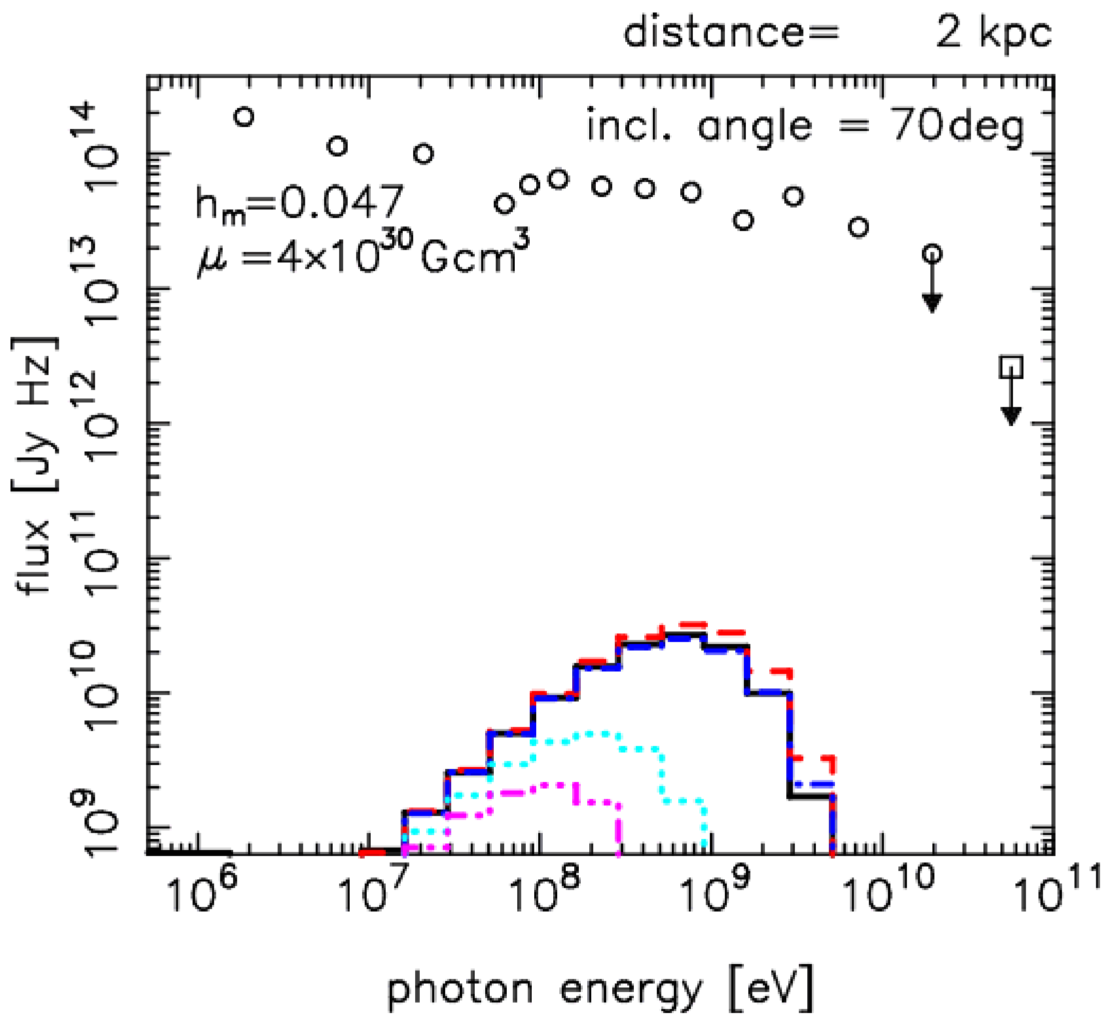

§4 *Crab Pulsar: super-GJ current solution*

As the gap becomes thicker, it becomes non-vacuum.
(i.e., created current > Goldreich-Julian value)

→ Inner part is substantially screened.

$h_m = 0.048$, $\alpha = 70^o$

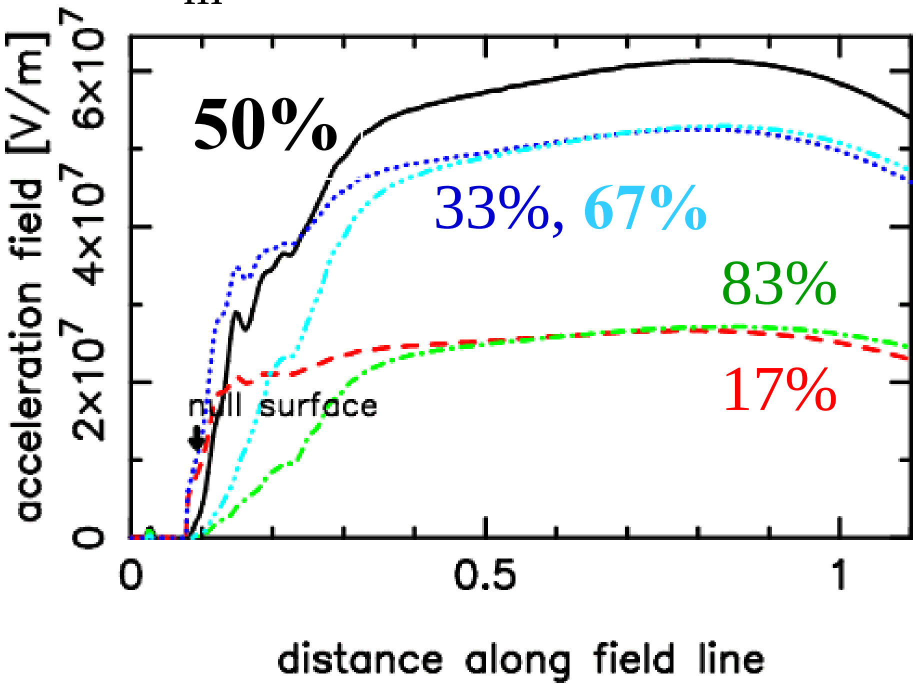

$h_m = 0.060$, $\alpha = 70^o$

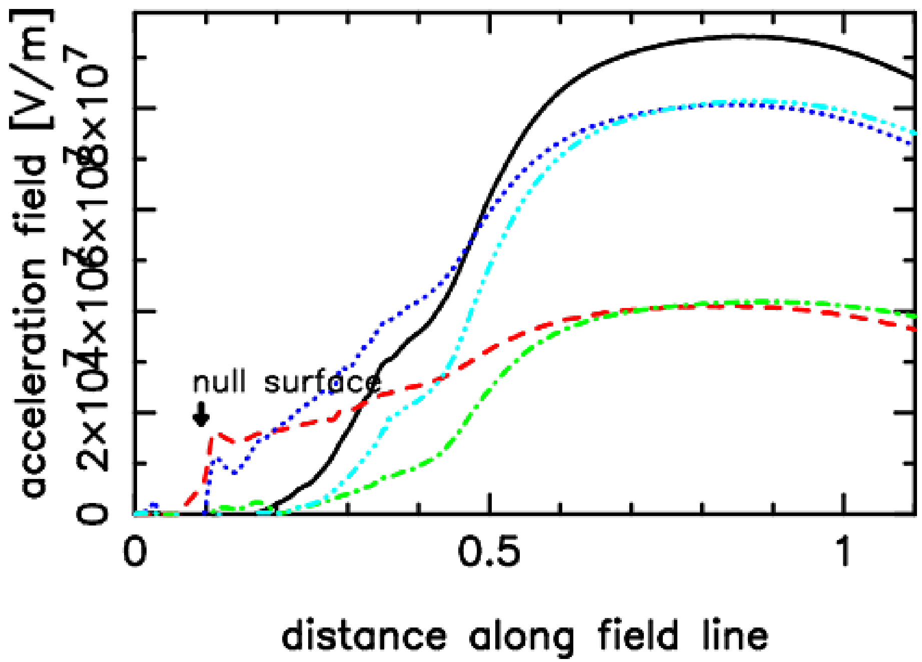

§4 real and GJ charge densities

$E_{\parallel} \sim 0$ because of the discharge of created pairs.

$\alpha = 70^{o}$

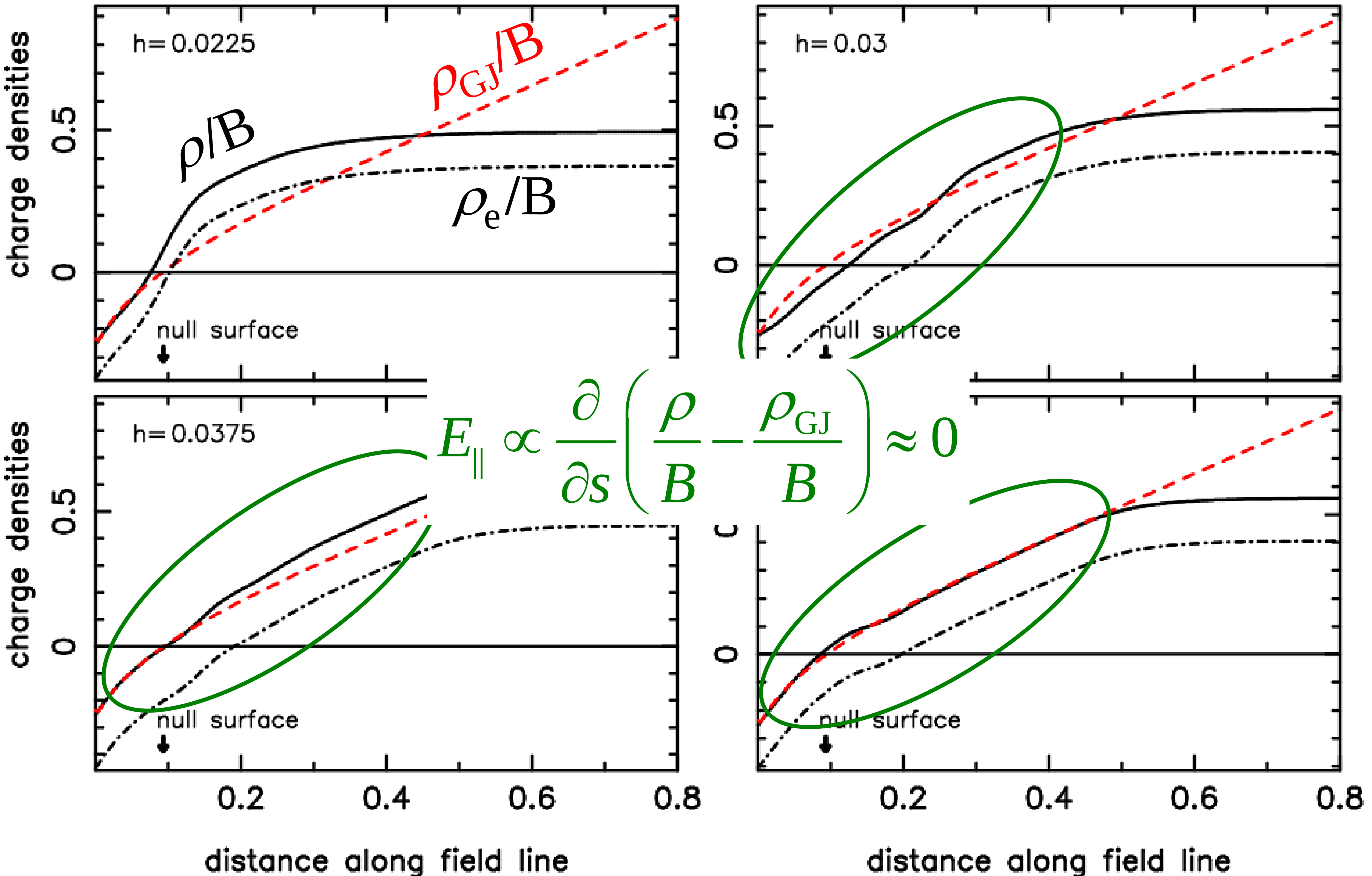

$$E_{\parallel} \propto \frac{\partial}{\partial s}\left(\frac{\rho}{B} - \frac{\rho_{GJ}}{B}\right) \approx 0$$

§4 super-GJ solution: flat spectrum

Super-GJ solution (new solution) predicts flat γ-ray spectrum below 100 MeV for transversely thick gap.

Crab pulsar spectrum

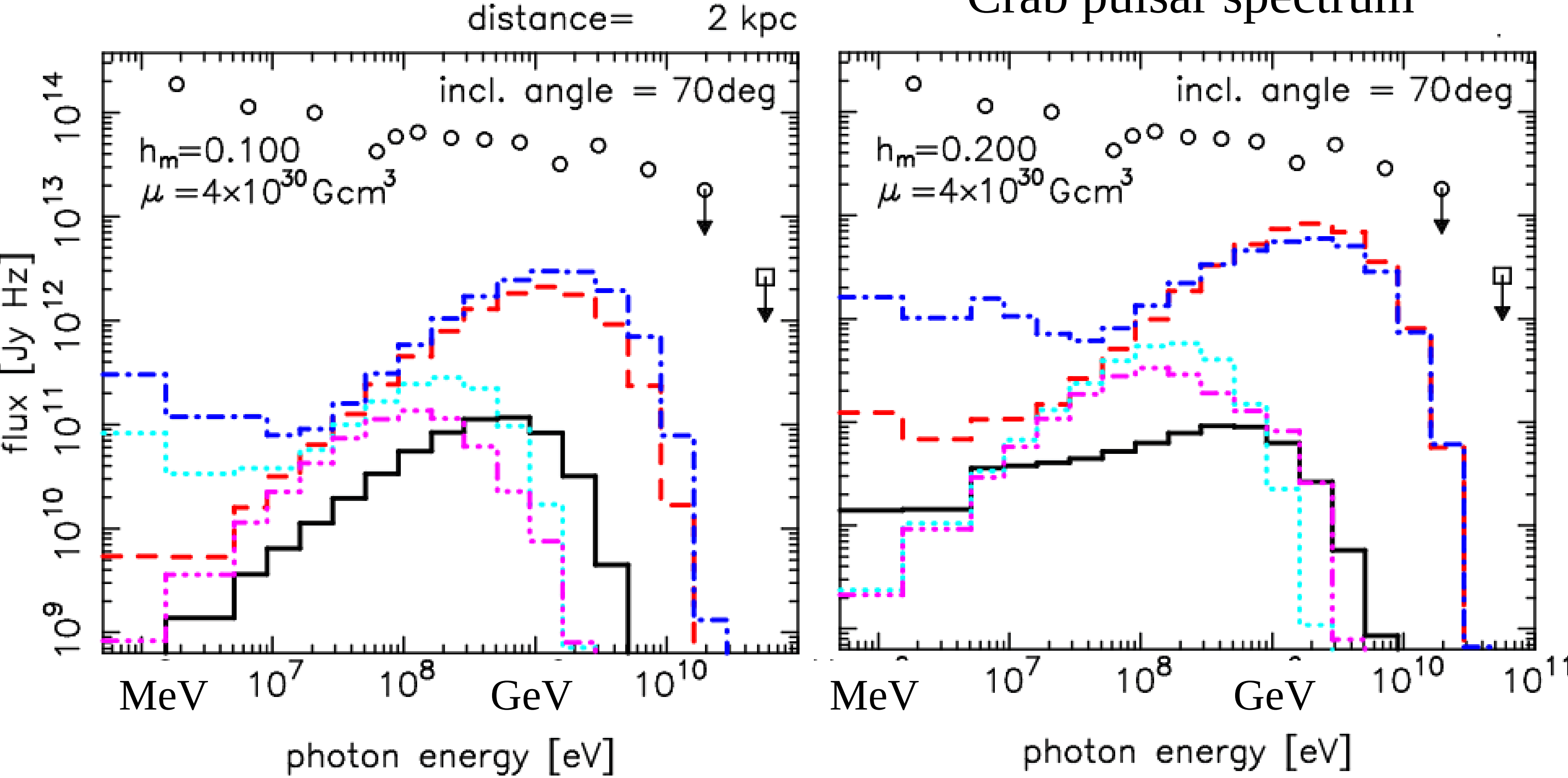

§5 *Discussion*

Let us compare this new solution with existing models.

Solving the same basic eqs. for the same pulsar under similar BDCs, Muslimov & Harding (2004) obtained a different solution in their polar-slot gap model.

They considered a space-charge-limited flow, which consists of only electrons extracted from NS surface.

§5 Discussion

Without pair creation, electron density per B will be constant along the field line. However, it results in a reversal of $E_{\|}$ due to the sign change of $\rho - \rho_{GJ}$.

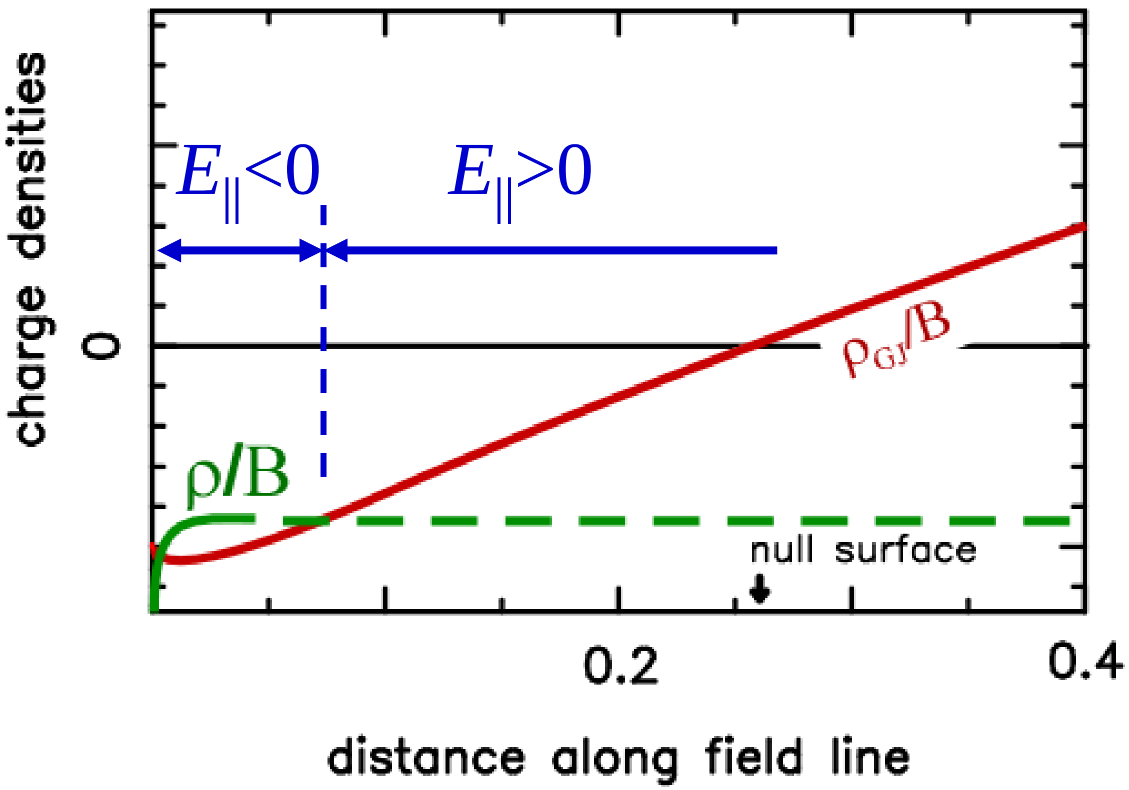

§5 Discussion

To avoid the reversal of $E_{\parallel}$ sign, they assumed that ρ/B changes in the same manner as ρ_{GJ}/B.

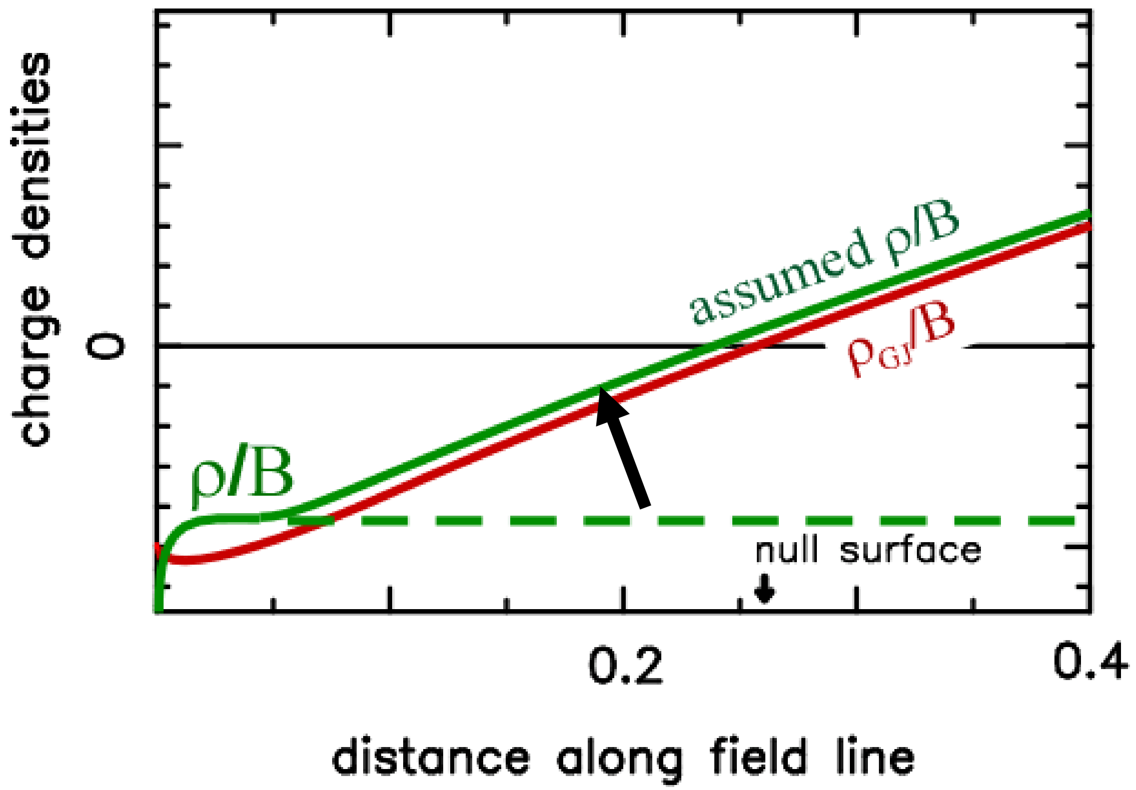

§5 Discussion

Because of this small $(\rho - \rho_{GJ})/B$, weak $E_{||}$ appears in the slot gap.

This weak $E_{||}$ results in a less efficient pair creation and guarantees the completely-charge-separated-flow approx.

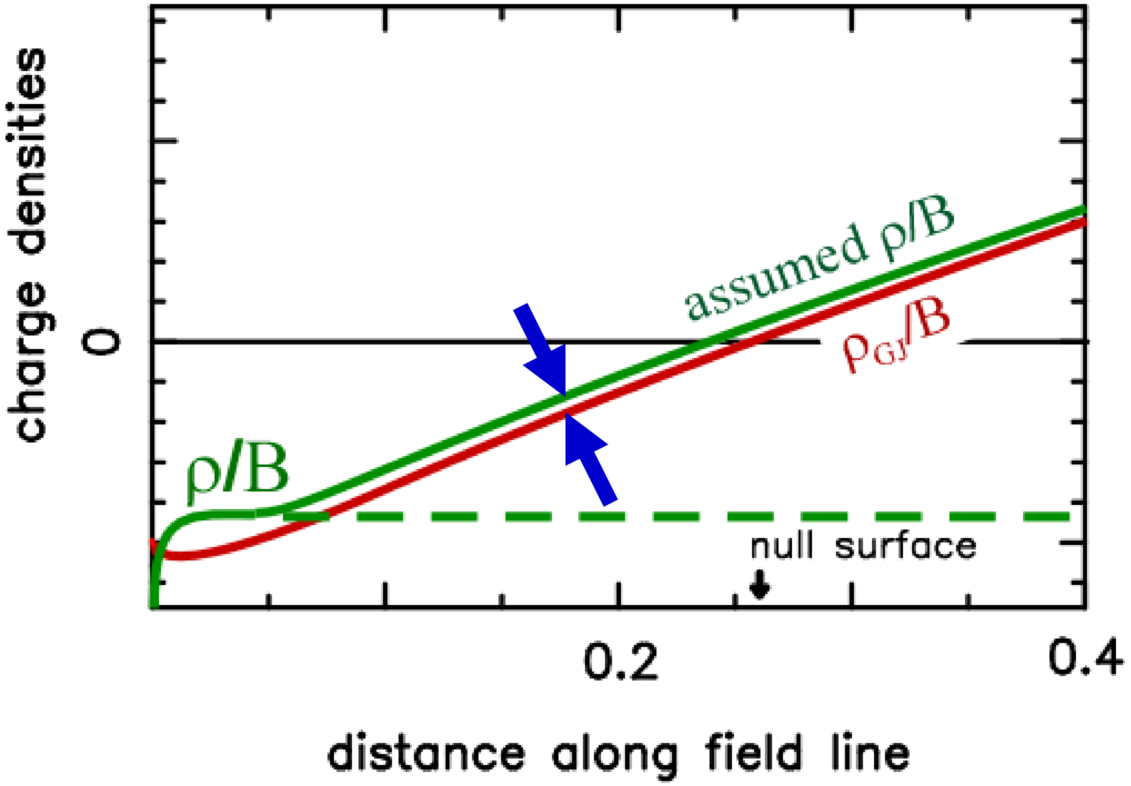

§5 Discussion

In short,

If $(\rho - \rho_{GJ})/B$ is a small positive constant without pair creation by some mechanism for a sub-GJ current, slot-gap solution becomes MH04 way with negative $E_{\parallel}$, extracting electrons from NS surface,

On the other hand,

If $(\rho - \rho_{GJ})/B$ is a small negative value with pair creation by the discharge of created pairs for a super-GJ current, slot-gap solution becomes this-work way with positive $E_{\parallel}$, extracting ions from NS surface.

Summary

- A stationary pair-creation cascade in pulsar magnetospheres is self-consistently solved from the set of Maxwell & Boltzmann eqs. on 2-D poloidal plane.

- A thin gap gives a traditional outer-gap solution (e.g., constant positive $E_{||}$). Crab γ-ray flux is negligible

- A thick gap gives a super-GJ current solution. $E_{||}$ is substantially screened in the inner part due to the discharge of created pairs. Crab γ-ray spectrum is flat.

- Super-GJ solution is a mixture of traditional inner- and outer-gap models (charge emission + $E_{||}$>0).

- It is ρ/B that determines if the solution becomes this-work way (copious pair creation, $E_{||}$>0, ion emission) or polar-slot-gap way (no pair creation, $E_{||}$<0, e^- emission).

§4 New gap model: Boundary conditions

To solve the set of Maxwell & Boltzmann equations, we must impose appropriate BCs.

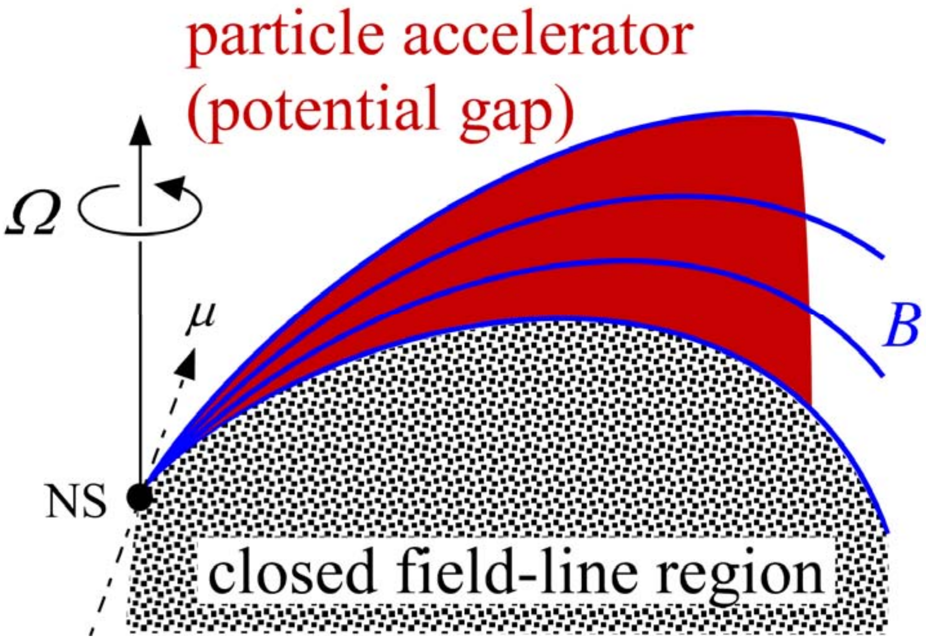

Assume that…

inner boundary
= stellar surface

lower boundary
= last-open field line

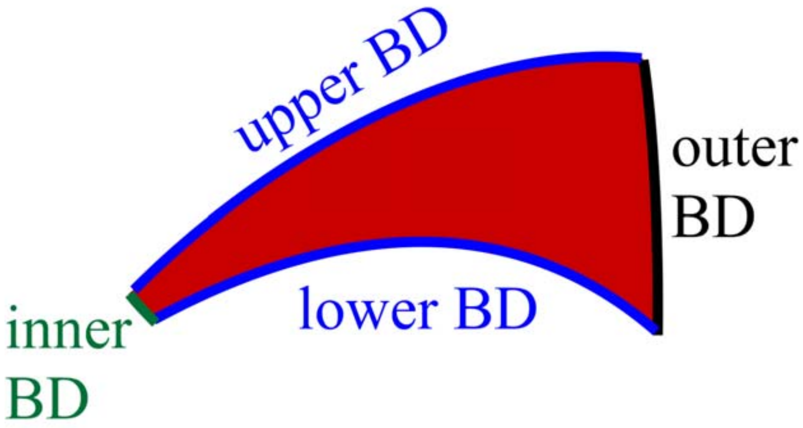

§4 New gap model: Boundary conditions

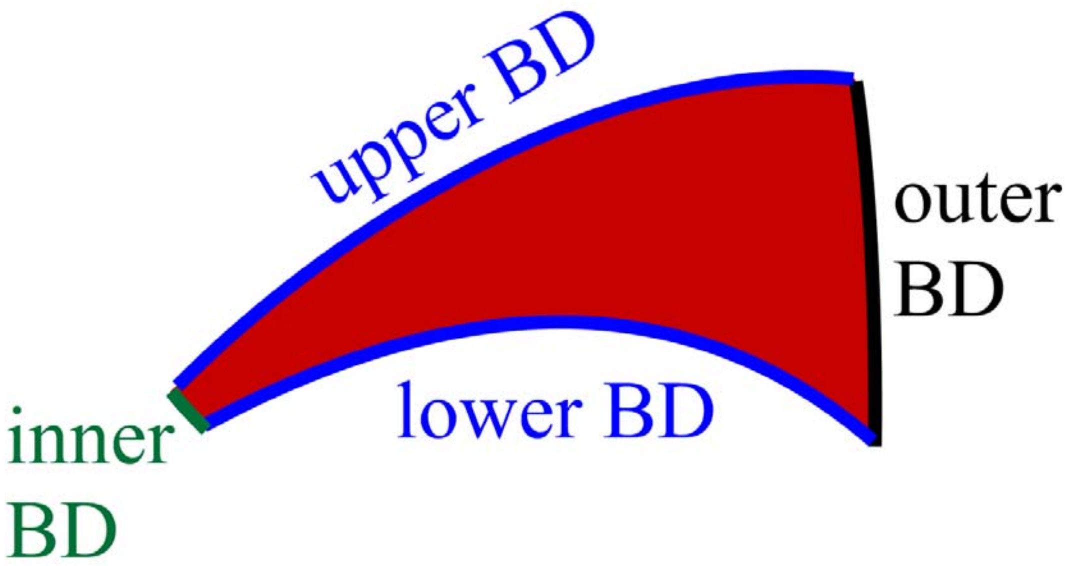

To solve the Poisson eq. for electrostatic potential Ψ, we impose

$$\Psi = 0 \qquad \text{at inner, lower, upper BDs}$$

$$\frac{\partial \Psi}{\partial x} = 0 \qquad \text{at outer BD}$$

§4 New gap model: Boundary conditions

To solve particle/γ-ray Boltzmann eqs., we assume that $e^-/e^+/\gamma$-rays are not injected across the **inner boundary**

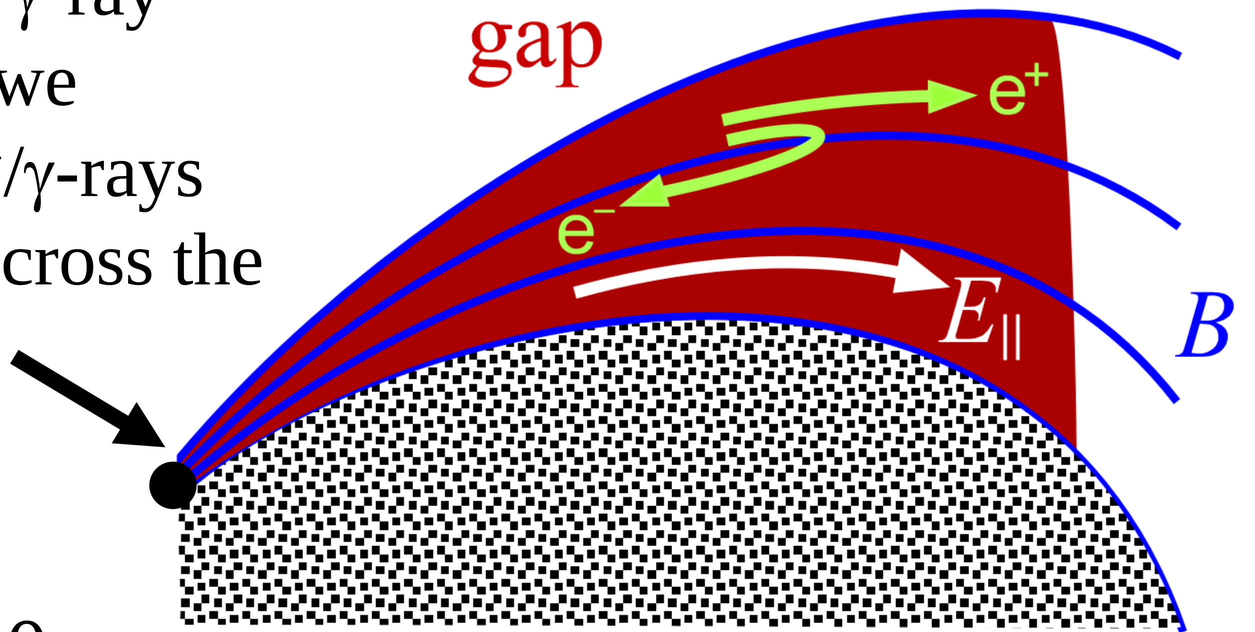

$$N_+(x^{\rm in}, z, \Gamma) = 0$$

$$G(x^{\rm in}, z, E_\gamma, \theta_\gamma) = 0, \quad \text{where } 0 < \theta_\gamma < \pi/2 \text{ (outgoing)}$$

§4 New gap model: Boundary conditions

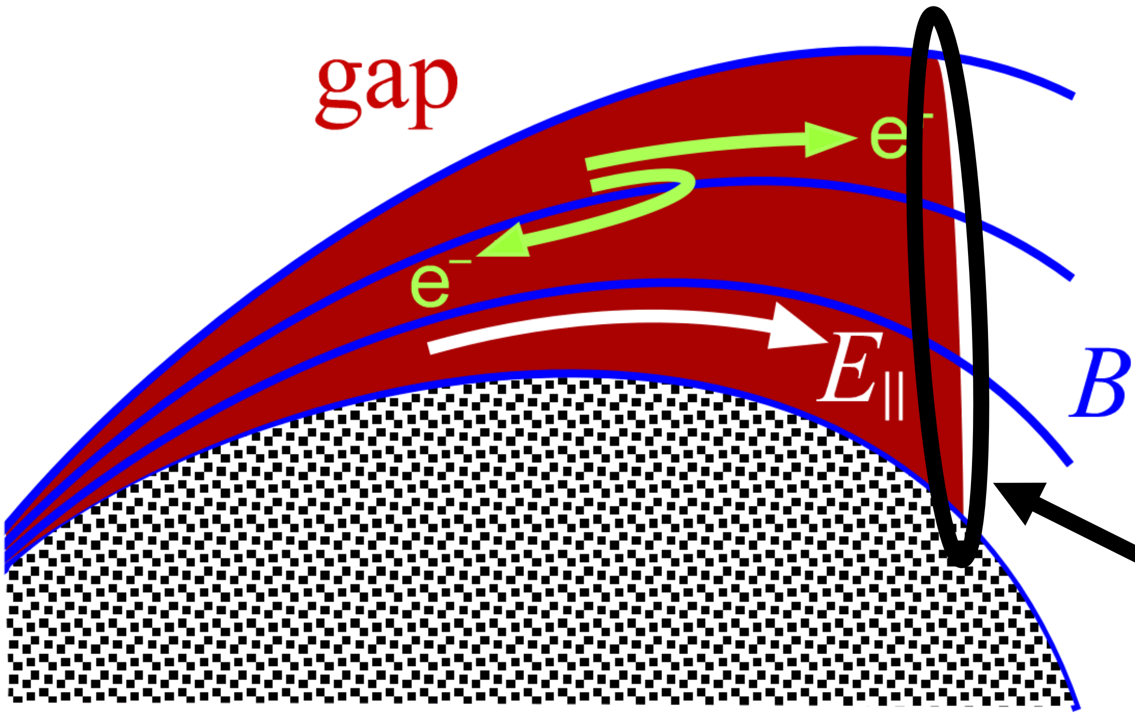

At the **outer boundary**, we also assume no injection of partilces/γ-rays.

$$N_{-}(x^{\mathrm{out}}, z, \Gamma) = 0$$

$$G(x^{\mathrm{out}}, z, E_\gamma, \theta_\gamma) = 0, \quad \text{where } \pi/2 < \theta_\gamma < \pi \text{ (in-going)}$$

That is, no particle/γ-ray injection across the BD.

§1 Introduction: CGRO observations

The OSSE/EGRET experiments have detected pulsed signals from 7+3 rotation-powered pulsars.

7 highest-confidence γ-ray pulsars
(statistical probability occurring by chance $< 10^{-9}$)

Crab	Nolan et al. 1993, ApJ 409, 697
B1509-58*	Matz et al. 1994, ApJ 434, 288
Vela	Kanbach et al. 1994, A&A 289, 855
Geminga	Mayer-Hasselwander et al. 1994, ApJ 421, 276
B1951+32	Ramanamurthy et al. 1995, ApJ 447, L109
B1706-44	Thompson et al. 1996, ApJ 465, 385
B1055-52	Thompson et al. 1999, ApJ 516, 297
Crab, Vela, Geminga	Fierro et al. 1998, ApJ 494, 734

* with OSSE

2D MHD wind model

Komissarov & Lyubarksy 2004

• Formation of torus in equatorial flow

• initial σ_0~10 - 100 is acceptable

• widely accepted value σ_0~10^4 gives too thick equatorial totus (100 times larger)

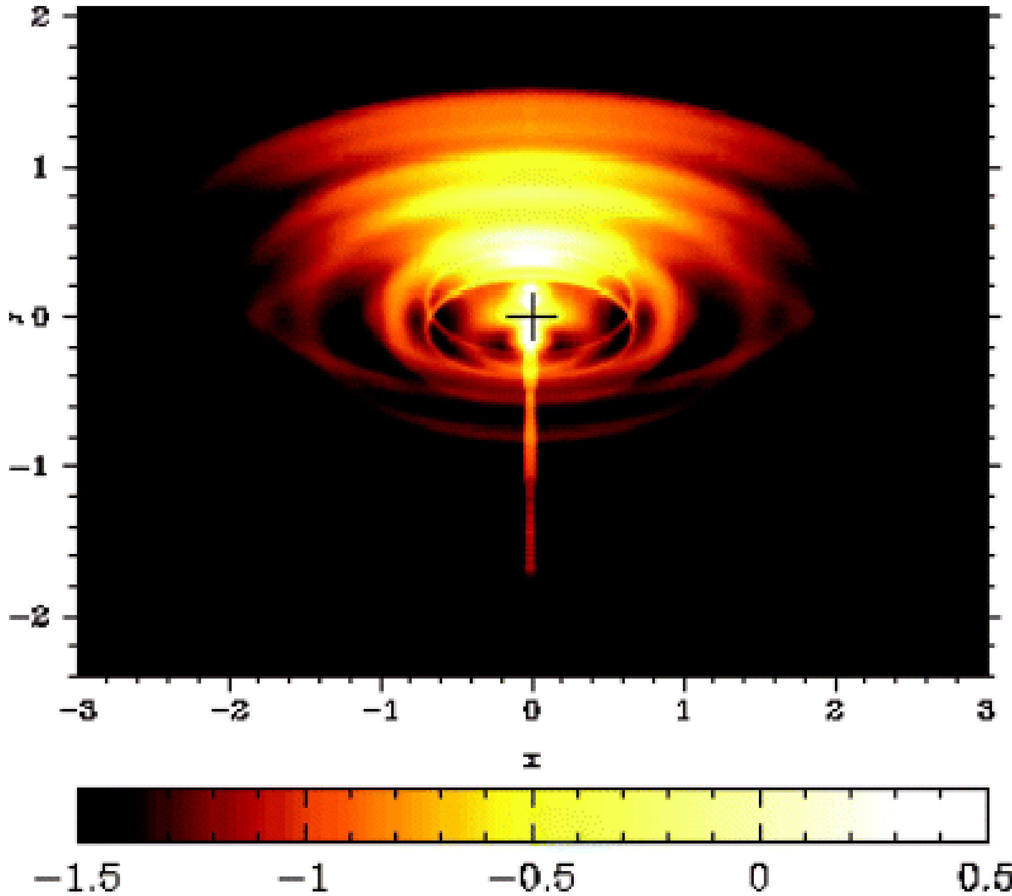

Compton Gamma Ray Observatory

EGRET on board CGRO

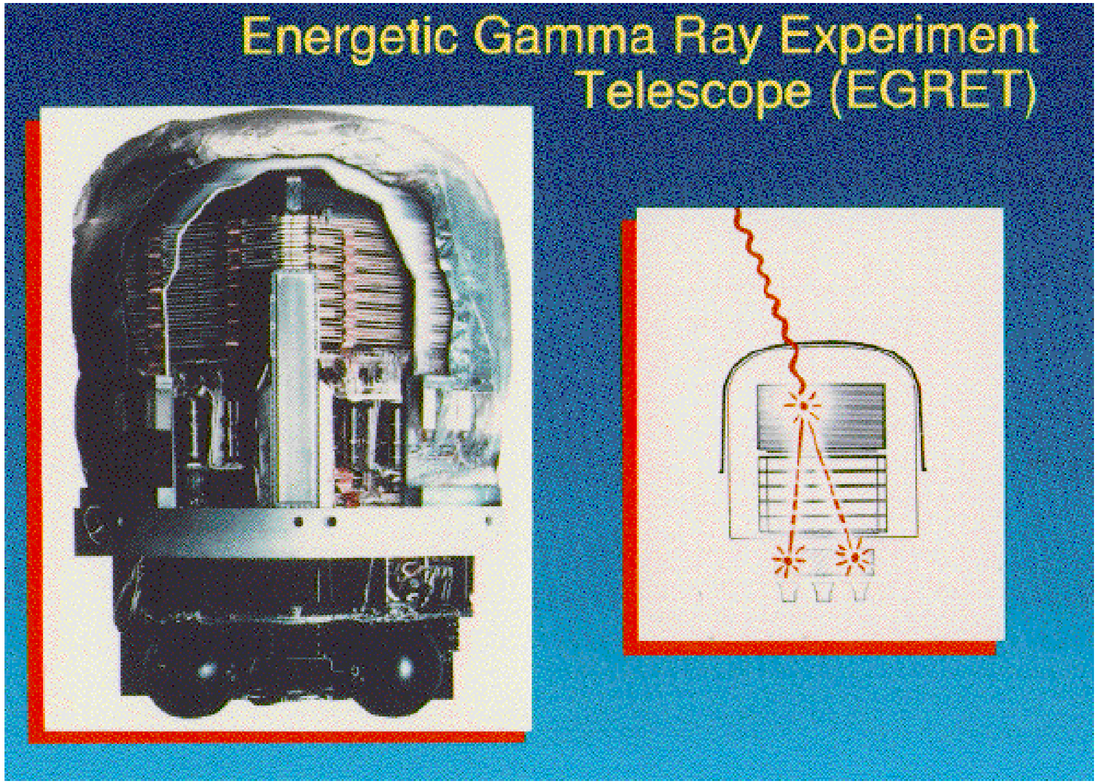

Energy range: 30 MeV to 30 GeV

Technique: high-voltage gas-filled spark chambers

Targets: diffuse γ-ray emission, γ-ray bursts, cosmic rays, pulsars, and blazars.

Cutoff energy vs. surface B field

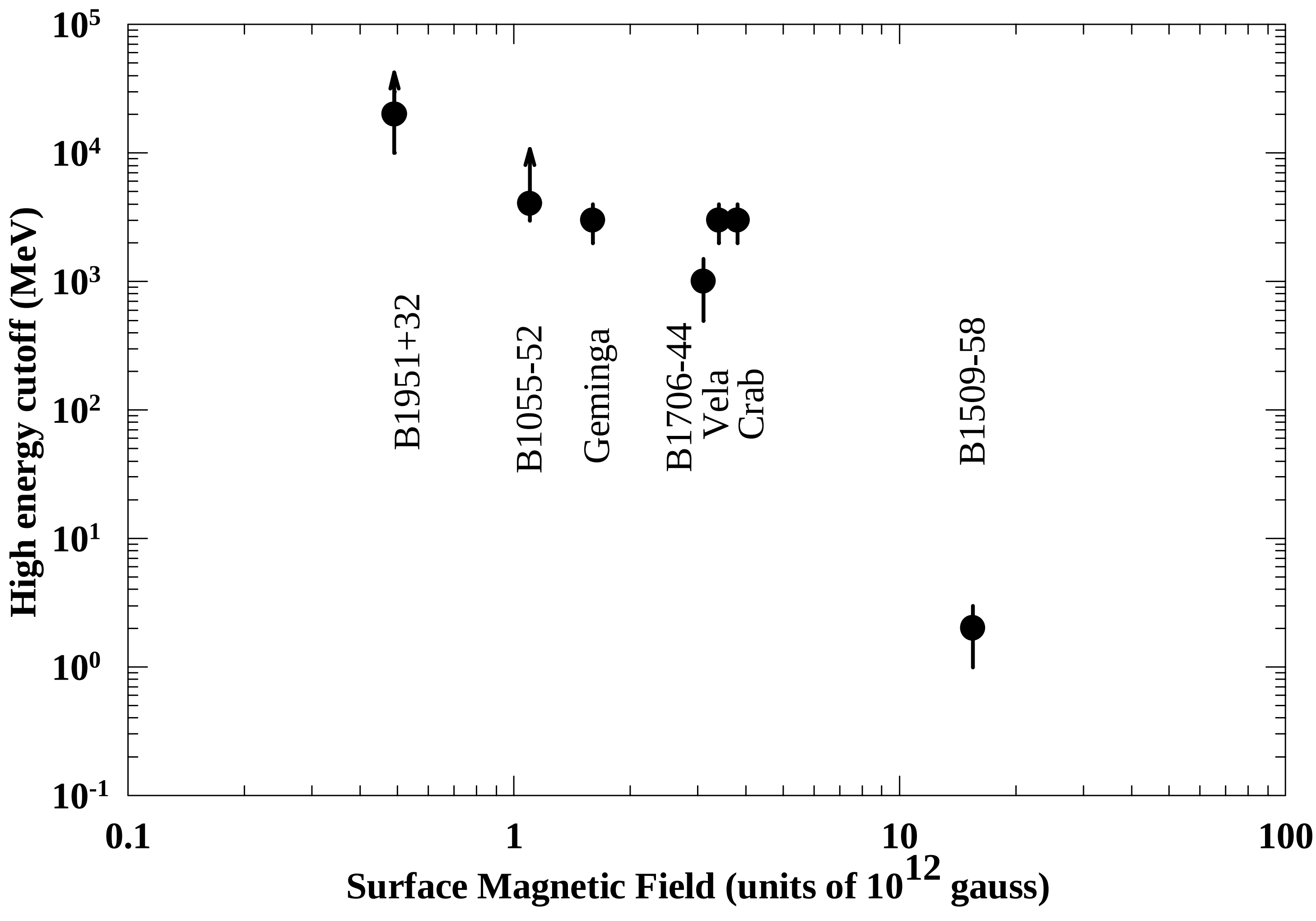

P-Pdot diagram

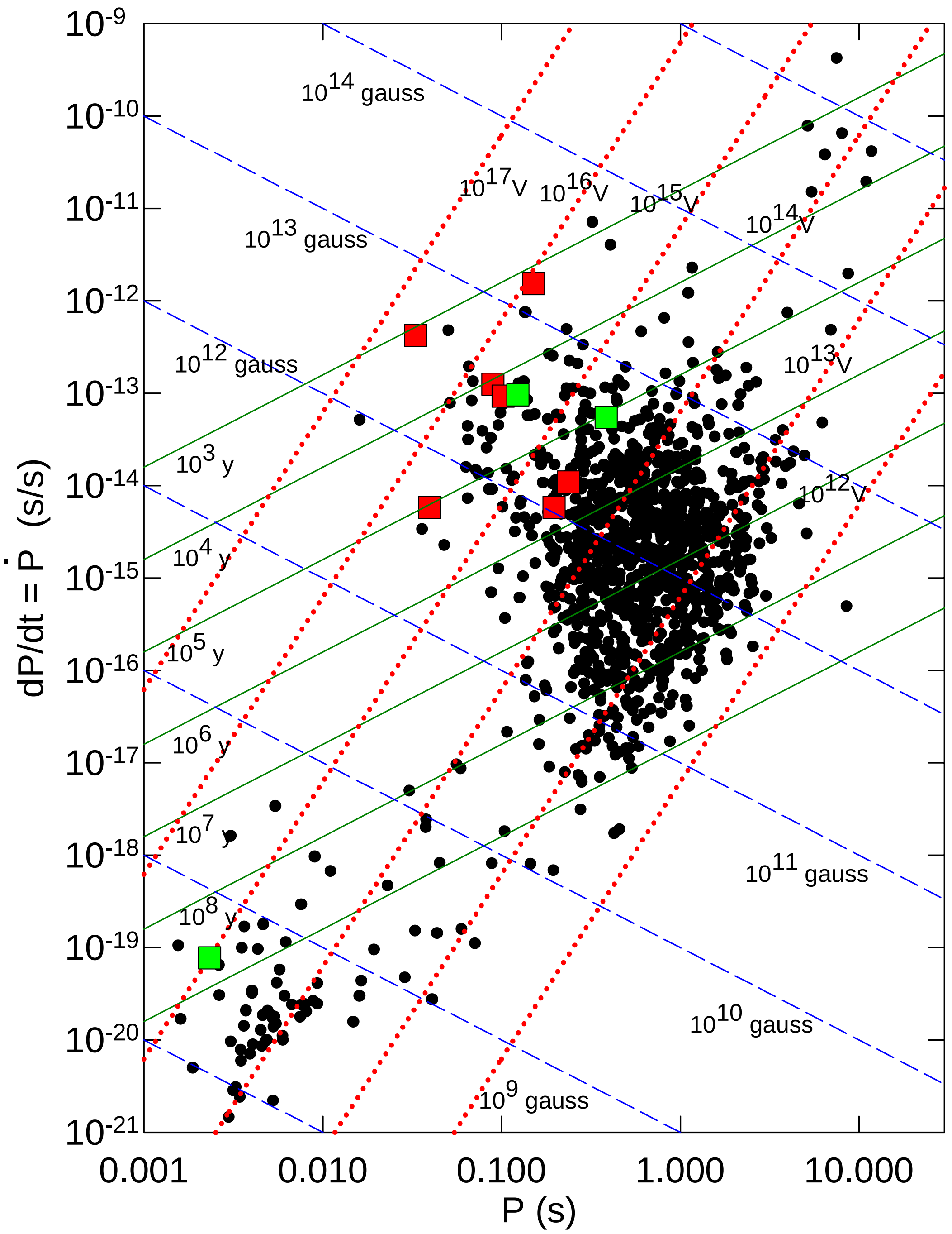

L vs L

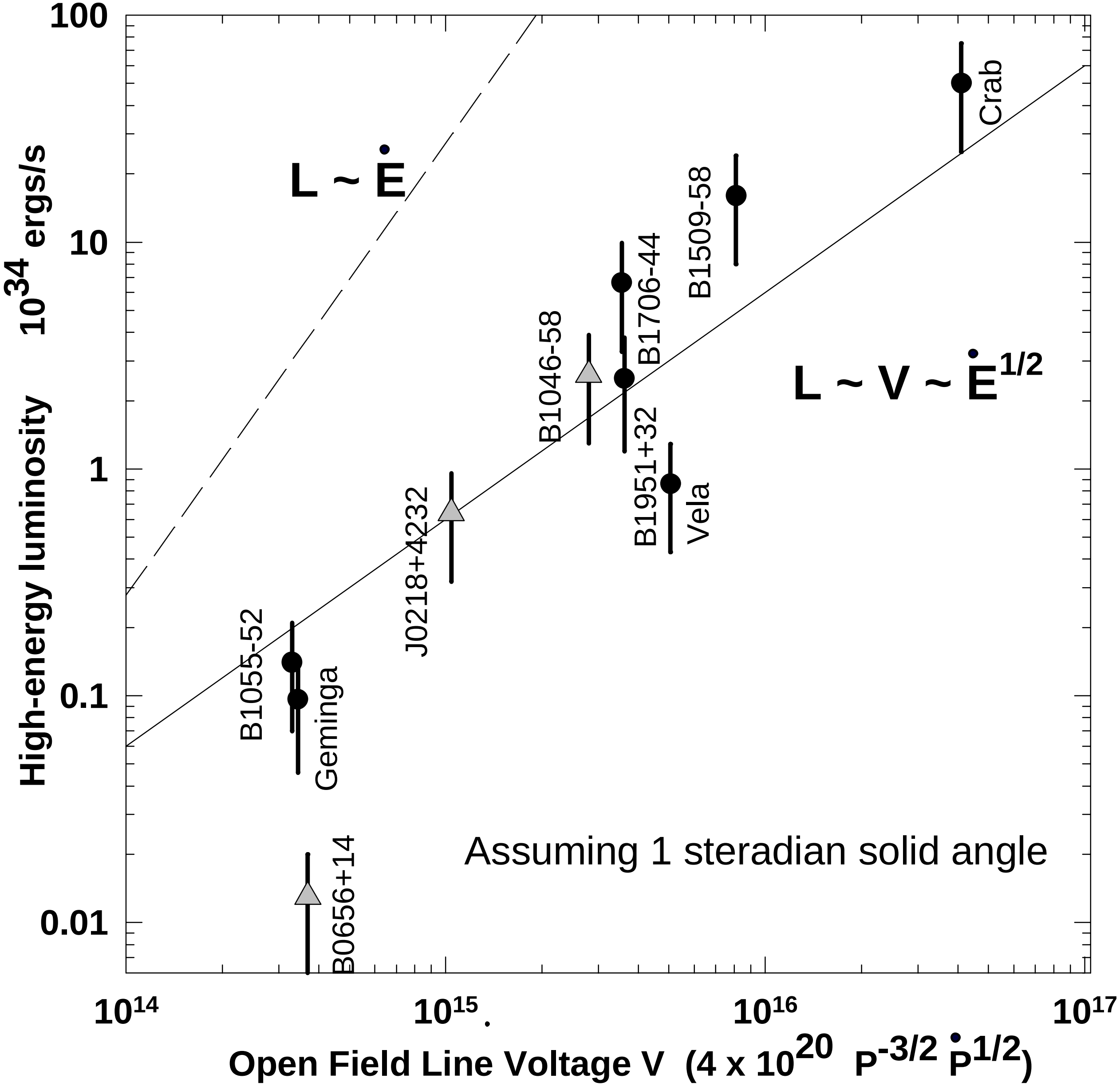

High-energy luminosity 10^{34} ergs/s
Open Field Line Voltage V (4 x 10^{20} P$^{-3/2}$ $\dot{P}^{1/2}$)
$L \sim \dot{E}$
$L \sim V \sim \dot{E}^{1/2}$
Assuming 1 steradian solid angle
Crab
B1509-58
B1706-44
B1046-58
B1951+32
Vela
J0218+4232
B1055-52
Geminga
B0656+14
100
10
1
0.1
0.01
10^{14}
10^{15}
10^{16}
10^{17}

Light curves: total vs. hard γ-rays

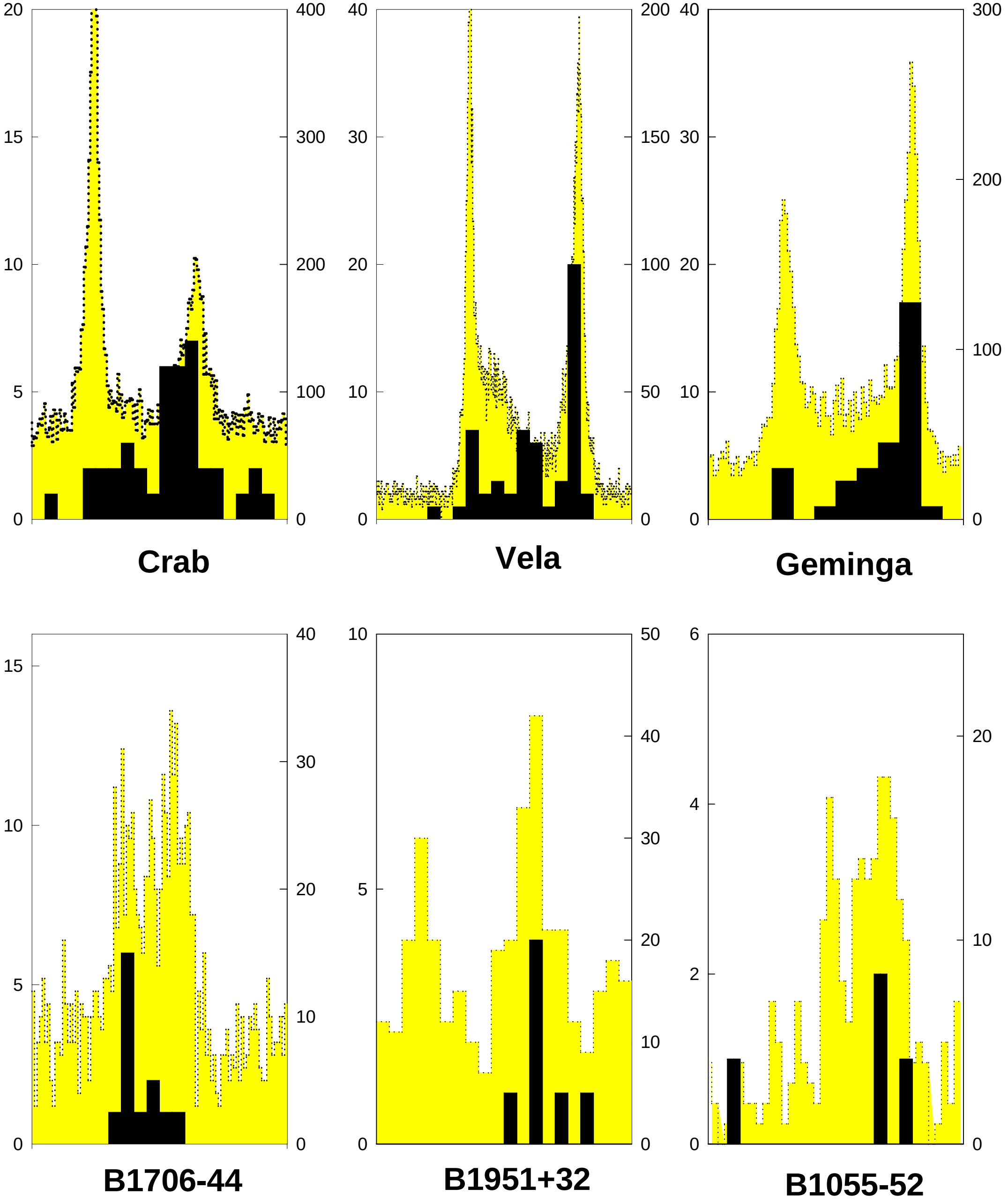

γ-ray pulsar observability

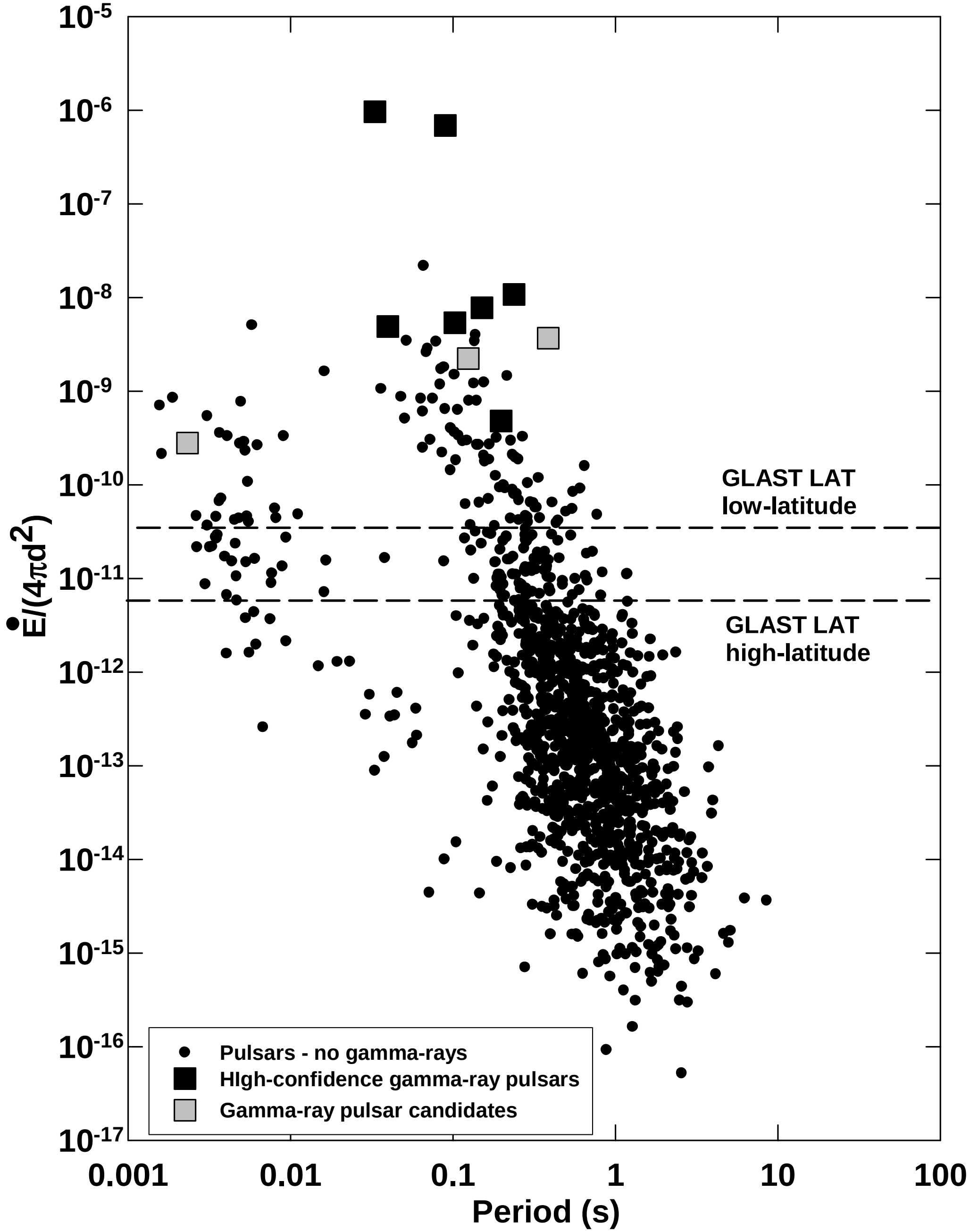

Seven highest-confidence γ-ray pulsars

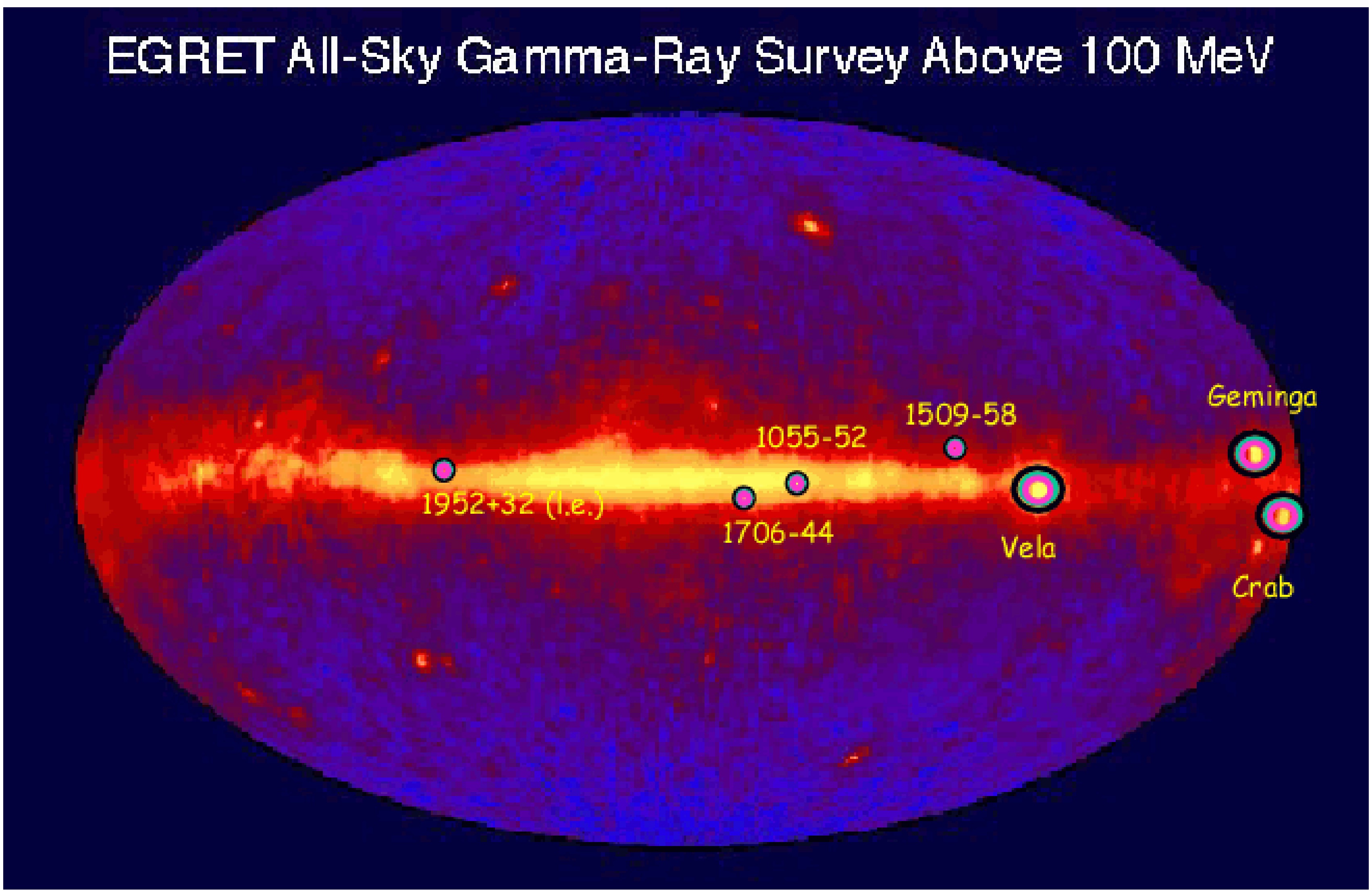

Multi-wavelength detections of high-energy pulsars

Table of detections

High-Energy Pulsars: Multiwavelength Detections								
PSR P	(ms)	$\dot{E}/d^2$ rank	radio	opt	X_{low}	X_{hi}	γ_{low}	γ_{hi}
high confidence γ-ray detections								
B0531+21 (Crab)	33.4	1 P		P	P	P	P	P
B0833-45 (Vela)	89.3	2 P		P	P	P	P	P
J0633+1746 (Geminga)	237.1	3 P?		P? P P	? P			
B1706-44	102.5	4	P ? D					P
B1509-58	150.7	5	P D P			P P		
B1951+32	39.5	6	P P P	P				
B1055-52	197.1	33 P		D P			P	P
candidate γ-ray detections								
B0656+14	384.9	18	P P P	? ?				
B0355+54	156.4	36	P		D	?		
B0631+10	287.7	53	P		D	?		
B0144+59	196.3	120	P	?				
candidate ms-PSR γ-ray detections								
J0218+4232	2.32	43	P		P	?		
B1821-24	3.05	14	P		P	?		
Likely PSR - γ-ray source positional coincidence								
B1046-58	123.7	8	P	D			D?	
J1105-6107	63.2	21	P	D			D?	
B1853+01	267.4	27	P	D?				

P = pulsed detection, P? = low significance pulsation, D = unpulsed detection

High-energy Lightcurves

High-Energy Lightcurves

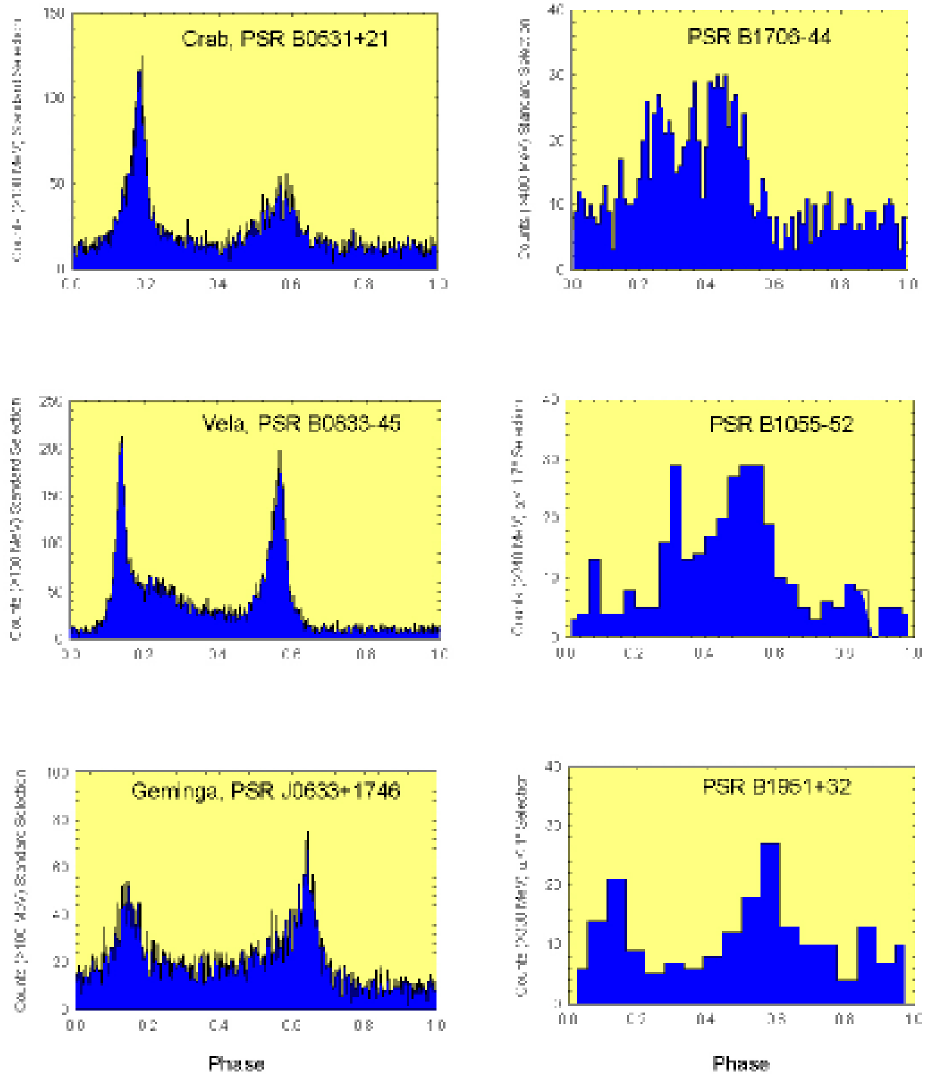

Multiwavelength Spectra of γ-ray Pulsars (pulsed emission)

- Maximum of Emission in the hard X- and γ-ray range
- High energy spectral cut-off
- Distinct spectral components

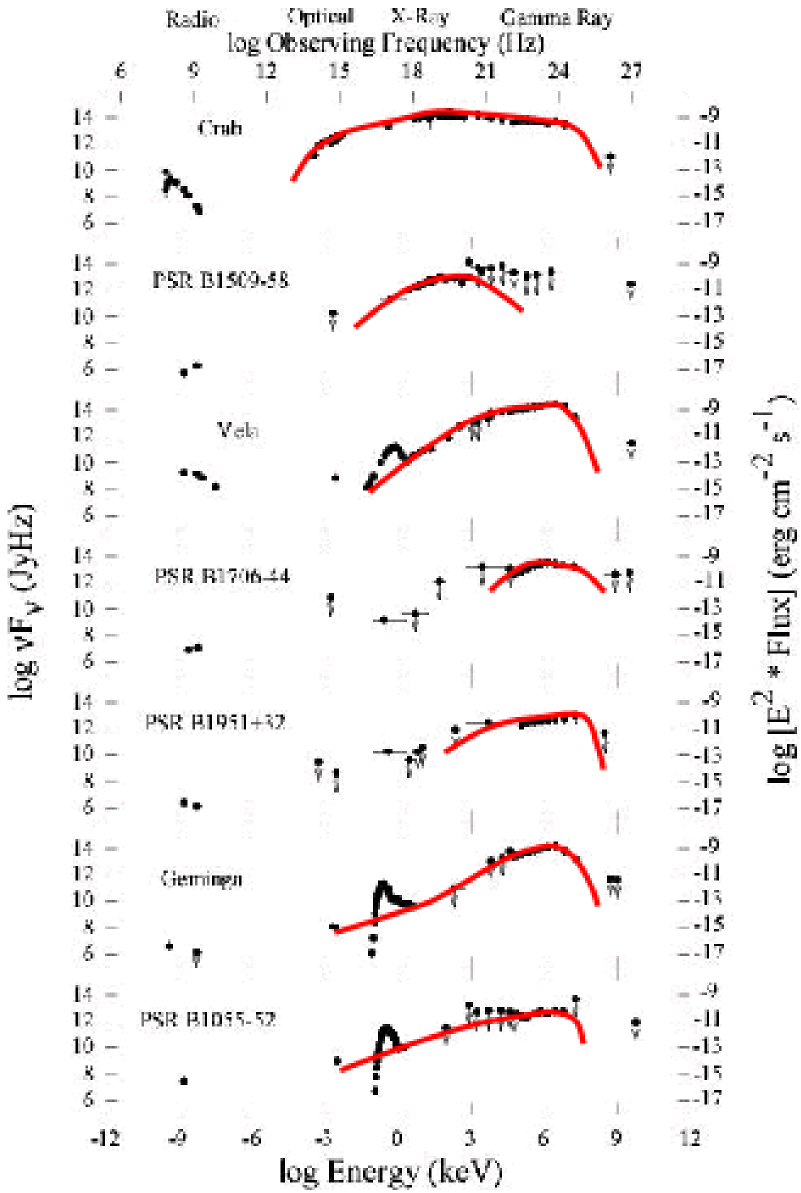

Summary of Observational Results for γ-Pulsars

Lightcurves:

- m ost γ-ray lightcurves show double peaks but extra components (bridges, smaller peaks) are often present

Spectra:

- power laws between 100 MeV and few GeV: indices between 1.2 (old PSR) and 2.2 (young PSR)
- strong spectral cut-offs (most at at a few GeV, but PSR1509-58 at ~30 MeV)

Luminosity and Efficiency:

- apparent luminosity: 10^{33} –1 0^{36} erg/s;
- γ -ray efficiency increases with PSR age
- pulsars are constant γ -ray sources

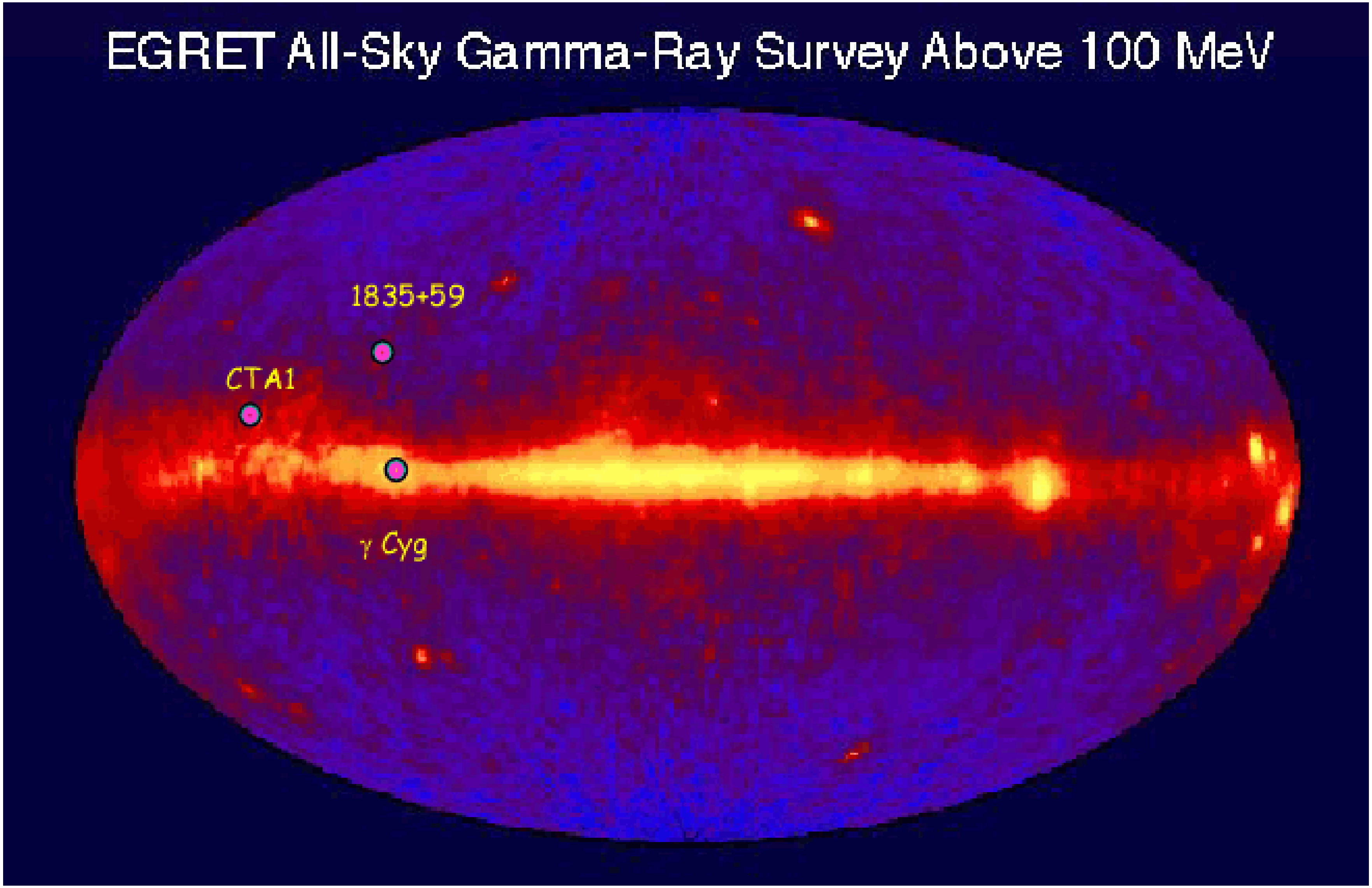
EGRET All-Sky Gamma-Ray Survey Above 100 MeV
1835+59
CTA1
γ Cyg

γ Cyg Chandra Search:
Becker et al., 2004, subm. to ApJ

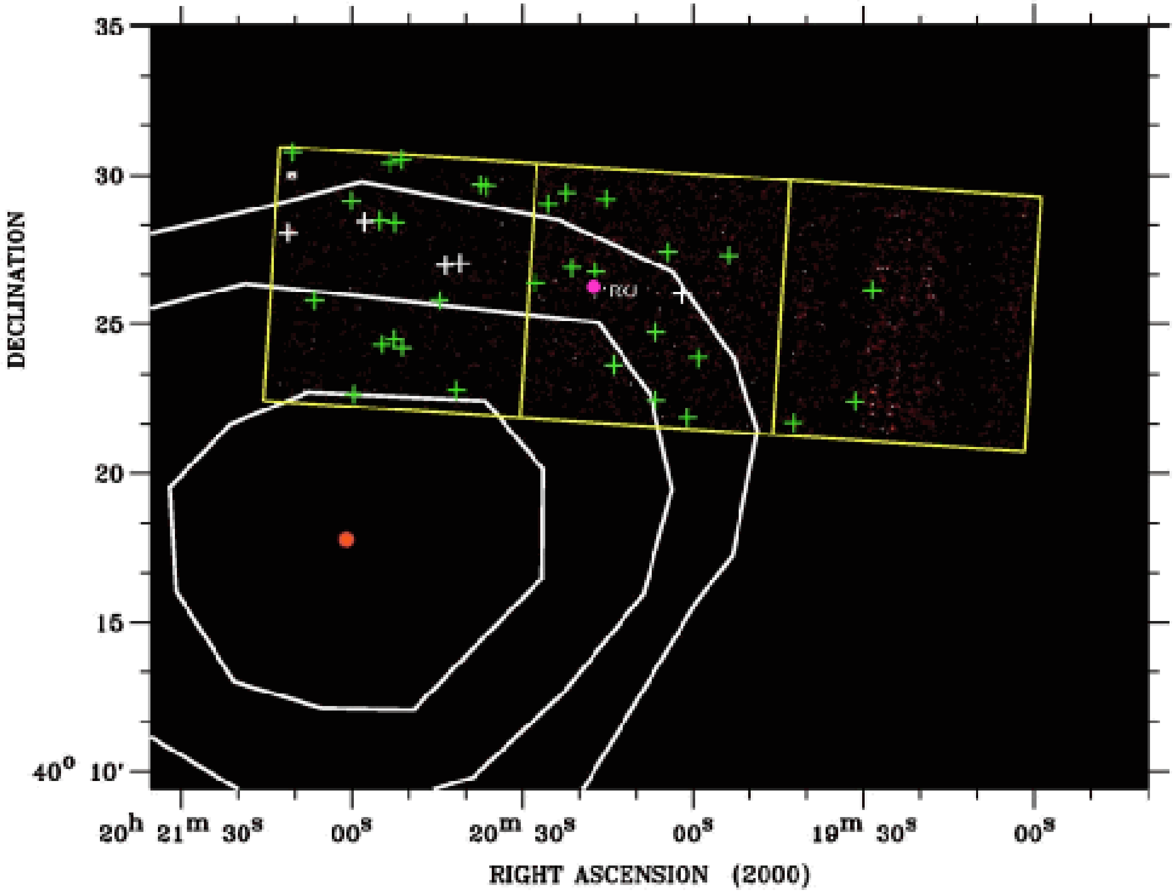

37 new X-ray sources discovered (30ks obs.)

The RXJ source is coincident with the K0V star.

Most sources are stars

γ Cyg: ROSAT PSPC/HRI

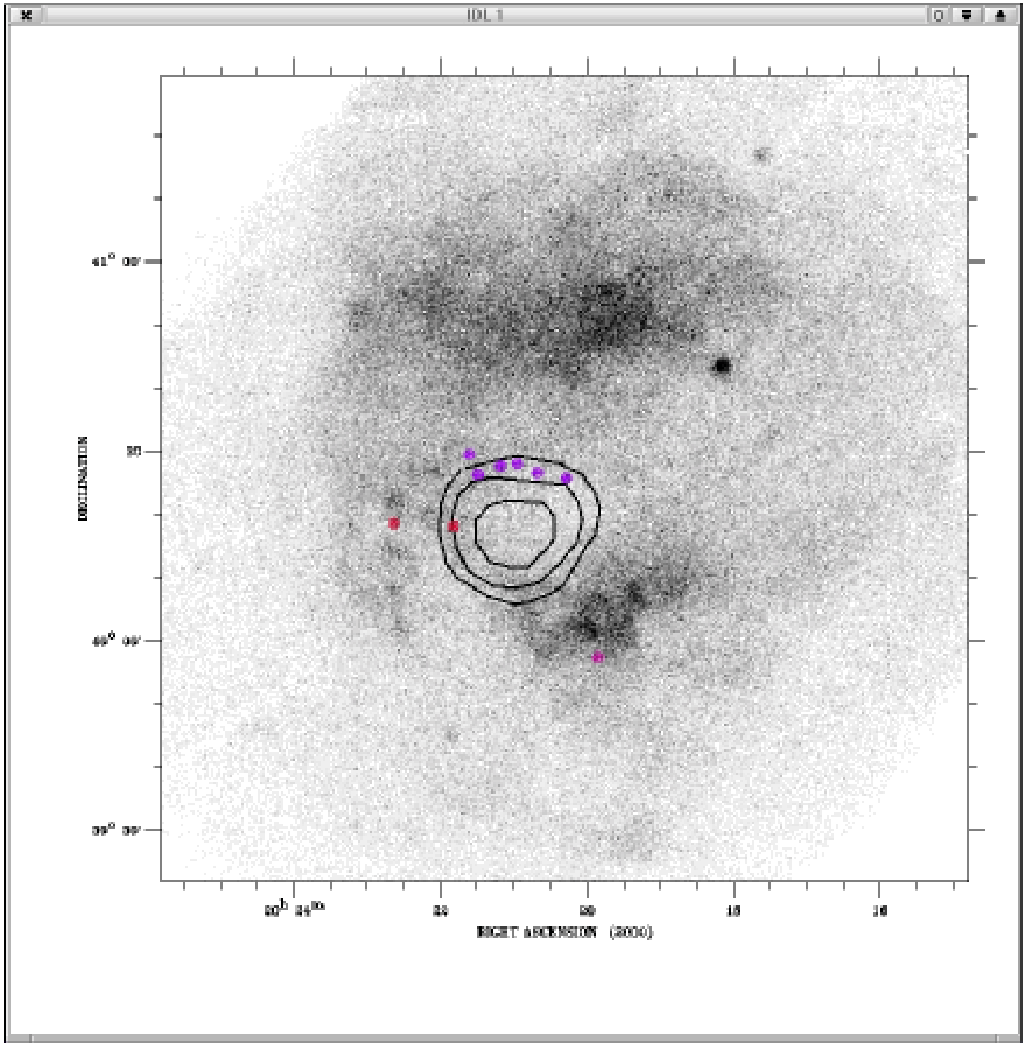

Reanalysis of ROSAT HRI fields:
9 sources found

6 common with Chandra
of which 2 seem variable

Conclusions on γCyg, 3EG J1835+59, CTA 1:

All three gamma-ray sources harbour X-ray counterparts that indicate possible ‚Geminga' like pulsars. Ratio Gamma/X is above severaL thousand.

In CTA 1 a plerion seems to be present

No radio or unique optical counterparts are found

Multiwavelength searches will continue (mainly in X-rays) in order to find periodicities.

With GLAST observations (after 2007) the gamma-ray data alone will be sufficient to search for periodicities.

Catalog of Gamma-Ray-Sources

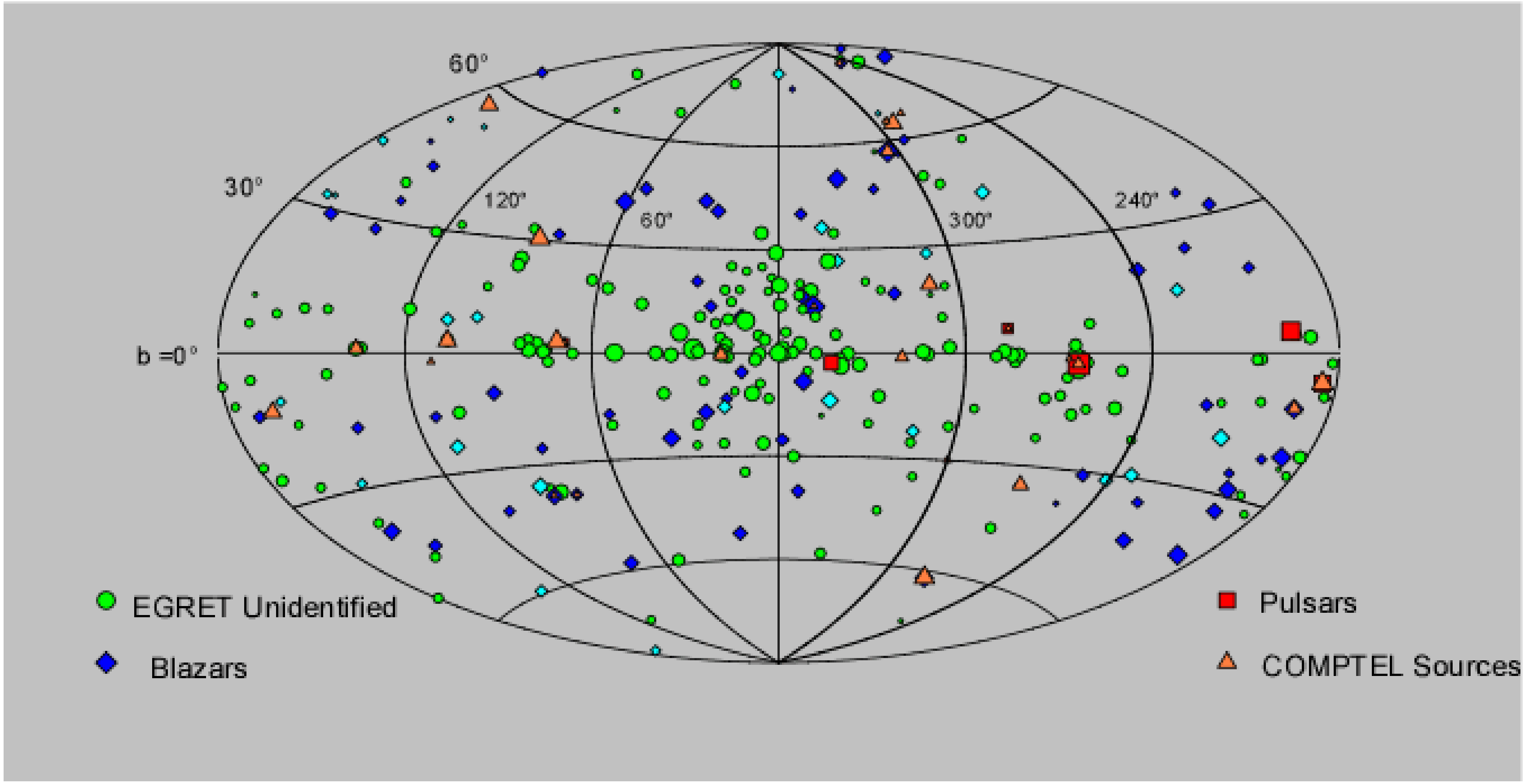

3. EGRET Catalog: (3EG) Hartman et al, 1999 ApJS, 123, 79	271 Sources 80-90 AGN 6-8 PSR ~170 Unid..	1. COMPTEL Katalog: Schönfelder et al., 2000 A&AS, 143, 145	32 constant Srces. 39 transient 11 AGN 3 PSR 4 EGRET Unid.

> 100 MeV Spectra of unidentified galactic sources

About 1/3 of the unidentified sources have hard ‚pulsarlike' spectra

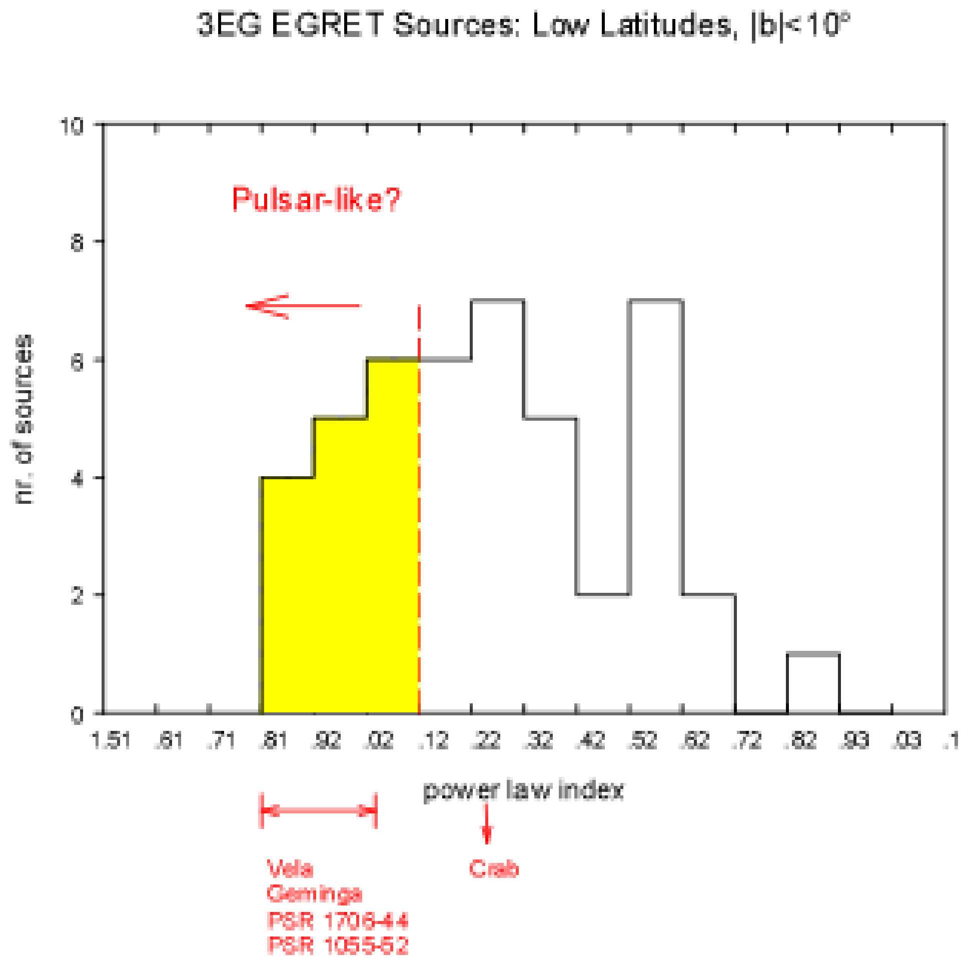

Conclusions on Unidentified Sources

Spatial and Flux Analysis of low latitude srcs:

$6\times10^{34} < L_{>100\ MeV} < 4\times10^{35}$ erg/s ; D ~ 1-5 kpc

Total nr. of sources in Galaxy: 700-3400 → 10-20% L_{gal}

N.B. Pulsar Luminosities: *Geminga* 1.5×10^{34} erg/s *Crab* 7×10^{35} erg/s

Spectral Analysis:

About 30% of the galactic sources have a hard, pulsar-like, spectrum

Temporal Analysis:

Galactic Sources with hard spectra are less variable than soft spectrum sources

Local System at medium latitudes: (Grenier, 1999; Gehrels et al., 2000)

Gould's Belt: starforming regions with h.e. sources
D ~ 100-500 pc $L_\gamma \sim 10^{32}-10^{33}$ erg/s